

Parsimonious mixtures of multivariate contaminated normal distributions

Antonio Punzo^{a,*}, Paul D. McNicholas^b

^a *Department of Economics and Business, University of Catania, Catania, Italy.*

^b *Department of Mathematics & Statistics, McMaster University, Hamilton, Canada.*

Abstract

A mixture of multivariate contaminated normal distributions is developed for model-based clustering. In addition to the parameters of the classical normal mixture, our contaminated mixture has, for each cluster, a parameter controlling the proportion of mild outliers and one specifying the degree of contamination. Crucially, these parameters do not have to be specified *a priori*, adding a flexibility to our approach. Parsimony is introduced via eigen-decomposition of the component covariance matrices, and sufficient conditions for the identifiability of all the members of the resulting family are provided. An expectation-conditional maximization algorithm is outlined for parameter estimation and various implementation issues are discussed. Using a large scale simulation study, the behaviour of the proposed approach is investigated and comparison with well-established finite mixtures is provided. The performance of this novel family of models is also illustrated on artificial and real data.

Keywords: Contaminated normal distribution, contamination, EM algorithm, mixture models, model-based clustering.

1. Introduction

Mixtures of multivariate normal distributions have been extensively considered as a powerful device for clustering by typically assuming, as we do, that each mixture component represents a cluster (or group or class; cf. McLachlan and Basford, 1988, Fraley and Raftery, 1998, Böhning, 2000, and McNicholas, 2016). Their popularity is largely attributable to computational and theoretical convenience, as well as the speed with which these mixtures can be implemented for many data sets. The volume of published work on normal mixtures has increased significantly since the work of Banfield and Raftery (1993) and Celeux and Govaert (1995); the latter work completes the former by introducing a family of fourteen mixtures of multivariate normal distributions obtained by imposing some constraints on eigen-decomposed component covariance matrices.

Unfortunately, real data are often contaminated by outliers that affect the estimation of the component means and covariance matrices (see, e.g., Barnett and Lewis, 1994, Becker and Gather, 1999, Bock, 2002, and Gallegos and Ritter, 2009). Thus, outlier detection and the development of robust methods of parameter estimation insensitive to their presence are important problems (see García-Escudero and Gordaliza, 1999 and Hennig, 2004). Outliers are observations that deviate from the (posited) reference model (Aggarwal, 2013 and Hawkins, 2013), which is here assumed to be a mixture of multivariate normal distributions; for a discussion about the concept of reference model, see Davies and Gather (1993) and Hennig (2002). Outliers can be roughly distinguished into two types (cf. Ritter, 2015, pp. 79–80):

Mild outliers are sampled from some population different or even far from the assumed model. Such outliers generally reflect the difficulty of the model specification problem. In their presence, the statistician is recommended to choose a model flexible enough to accommodate all data points, including the outliers.

*Corresponding author: Email: antonio.punzo@unict.it, Phone: +39-095-7537640, Fax: +39-095-7537610
Email addresses: antonio.punzo@unict.it (Antonio Punzo), mcnicholas@math.mcmaster.ca (Paul D. McNicholas)

Gross outliers cannot be modelled by a distribution. They are unpredictable and incalculable. In the presence of gross outliers, the statistician is recommended to choose a method for suppressing them. A classical choice is trimming, introduced to cluster analysis by Cuesta-Albertos et al. (1997) and followed, only to cite a few, by Gallegos and Ritter (2005, 2009), García-Escudero et al. (2003, 2008, 2010), and Ruwet et al. (2013). The underlying idea is to decompose the data set into high-density regions, with the remainder consisting mainly of isolated observations (Hartigan, 1985). Of course, for this method to be effective the estimator must recognize the outliers automatically.

Mild outliers — also referred to as “bad” points herein, following Aitkin and Wilson (1980) — are the focus of this paper. For normal mixtures, they are often dealt using two approaches (cf. Ruwet et al., 2012). In the “additional component” approach, protection against outliers is obtained by adding a further convenient component distribution to the mixture of normal distributions to capture outliers. The first and most famous example in this direction is represented by the addition of a uniform component on the convex hull of the data, as suggested by Banfield and Raftery (1993); see also Hennig (2004) and Coretto and Hennig (2011) for the univariate case. In the “componentwise” approach, the component multivariate normal distributions are separately protected against outliers by using either convenient robust estimates of the means and covariance matrices (see Campbell, 1984, McLachlan and Basford, 1988, Section 2.8, De Veaux and Krieger, 1990, and Markatou, 2000) or, more often, by embedding them in more general heavy-tailed, usually elliptically symmetric, multivariate distributions. The classical example is the mixture of multivariate t distributions, which was first used for clustering by McLachlan and Peel (1998) and Peel and McLachlan (2000). Note that the multivariate t distribution can be written as a normal scale mixture, where the mixing weight is a gamma random variable; in fact, the multivariate normal distribution is a limiting case of the multivariate t distribution and the t distribution can be viewed as a generalization of the normal distribution (cf. Peel and McLachlan, 2000). A further example is given by Browne et al. (2012); they introduce a mixture model whereby each mixture component is itself a mixture of a normal and a uniform distribution. To have an idea of the data configurations where the “additional component” approach outperforms the “componentwise” approach, and *vice versa*, see the extensive simulation study reported by Coretto and Hennig (2015). Roughly speaking, the additional component approach is not expected to work well when the mild outliers are either cluster-dependent (Gerogiannis et al., 2009) or cannot be modeled adequately by the additional component (cf. McLachlan and Peel, 2000, p. 233).

By considering the “componentwise” approach, a mixture of multivariate contaminated normal distributions is proposed in Section 2.1. A multivariate contaminated normal distribution, which dates back to the seminal work of Tukey (1960), is a two-component normal mixture in which one of the components, with a large prior probability, represents the good observations (reference cluster distribution), and the other, with a small prior probability, the same mean, and an inflated covariance matrix, represents the bad observations (see also Aitkin and Wilson, 1980). It represents a common and simple theoretical model for the occurrence of bad points although, by construction, it cannot accommodate asymmetric contamination and/or “groups” of concentrated outliers. Furthermore, parsimonious variants of the proposed model are introduced, in the fashion of Banfield and Raftery (1993) and Celeux and Govaert (1995), by imposing constraints on eigen-decomposed component covariance matrices (Section 2.2). The model-based clustering framework is outlined (Section 2.3), and sufficient conditions for identifiability of our models are given (Section 3). An expectation-conditional maximization (ECM) algorithm for parameter estimation is outlined in Section 4. Further computational and operational aspects are discussed in Section 5. Advantageously, as it will be better explained in Section 5.6, once a mixture of multivariate contaminated normal distributions is fitted to the observed data, by means of maximum *a posteriori* probabilities, each observation can be first assigned to one of the clusters and then classified as good or bad. Moreover, as detailed in Section 5.5, bad points are automatically down-weighted in the estimation of the component means and covariance matrices. Thus, we have a model for simultaneous robust clustering and detection of mild outliers. Furthermore, the fact that all of the parameters can be estimated by maximum likelihood (see Section 4), and automatic criteria, such as the BIC (see Section 5.8), can be adopted to select the number of clusters and the parsimonious covariance structure (see Section 2.2),

implies that there is no need to preliminary visualize the data to try to understand what the outliers could be. This is the reason why our approach could be extended to higher dimensions where the visualization of the data becomes cumbersome. In Section 6, the behavior of the proposed model, in comparison with some of the approaches discussed above, is investigated through a large-scale simulation study. Applications on artificial and real data are presented in Section 7. The paper concludes with some discussion in Section 8.

2. Methodology

2.1. The general model

The distribution of a random vector \mathbf{X} , taking values on \mathbb{R}^p , according to a parametric finite mixture model, can be written as

$$p(\mathbf{x}; \boldsymbol{\psi}) = \sum_{g=1}^G \pi_g f(\mathbf{x}; \boldsymbol{\vartheta}_g), \quad (1)$$

where π_g is the mixing proportion for the g th component, with $\pi_g > 0$ and $\sum_{g=1}^G \pi_g = 1$, $f(\mathbf{x}; \boldsymbol{\vartheta}_g)$ is the density of the g th component with parameters $\boldsymbol{\vartheta}_g$, and $\boldsymbol{\psi} = \{\boldsymbol{\pi}, \boldsymbol{\vartheta}\}$, with $\boldsymbol{\pi} = \{\pi_g\}_{g=1}^G$ and $\boldsymbol{\vartheta} = \{\boldsymbol{\vartheta}_g\}_{g=1}^G$, contains all of the parameters of the mixture.

In this paper, for the g th mixture component, $g = 1, \dots, G$, we adopt the multivariate contaminated normal distribution

$$f(\mathbf{x}; \boldsymbol{\vartheta}_g) = \alpha_g \phi(\mathbf{x}; \boldsymbol{\mu}_g, \boldsymbol{\Sigma}_g) + (1 - \alpha_g) \phi(\mathbf{x}; \boldsymbol{\mu}_g, \eta_g \boldsymbol{\Sigma}_g), \quad (2)$$

where $\alpha_g \in (0.5, 1)$, $\eta_g > 1$, $\boldsymbol{\vartheta}_g = \{\alpha_g, \boldsymbol{\mu}_g, \boldsymbol{\Sigma}_g, \eta_g\}$, and

$$\phi(\mathbf{x}; \boldsymbol{\mu}, \boldsymbol{\Sigma}) = (2\pi)^{-\frac{p}{2}} |\boldsymbol{\Sigma}|^{-\frac{1}{2}} \exp\left\{-\frac{1}{2} \delta(\mathbf{x}, \boldsymbol{\mu}; \boldsymbol{\Sigma})\right\} \quad (3)$$

is the distribution of a p -variate normal random vector with mean $\boldsymbol{\mu}$ and covariance matrix $\boldsymbol{\Sigma}$. In (3), $\delta(\mathbf{x}, \boldsymbol{\mu}; \boldsymbol{\Sigma}) = (\mathbf{x} - \boldsymbol{\mu})' \boldsymbol{\Sigma}^{-1} (\mathbf{x} - \boldsymbol{\mu})$ denotes the squared Mahalanobis distance while $|\cdot|$ is the determinant. Note that α_g is constrained to be greater than 0.5 because, in robust statistics, it is usually assumed that at least half of the points are good; however, $\alpha_g \in (0, 1)$ is acceptable in general, as often happens in the literature. In (2), η_g denotes the degree of contamination, and because of the assumption $\eta_g > 1$, it can be interpreted as the increase in variability due to the bad observations (i.e., it is an inflation parameter; see Figure 1). Indeed, the covariance matrix in the g th component, $g = 1, \dots, G$, is given by

$$[\alpha_g + (1 - \alpha_g) \eta_g] \boldsymbol{\Sigma}_g, \quad (4)$$

where the scale factor satisfies the constraint $[\alpha_g + (1 - \alpha_g) \eta_g] > 1$ because $\eta_g > 1$. The density of our mixture of multivariate contaminated normal distributions is given by

$$p(\mathbf{x}; \boldsymbol{\psi}) = \sum_{g=1}^G \pi_g [\alpha_g \phi(\mathbf{x}; \boldsymbol{\mu}_g, \boldsymbol{\Sigma}_g) + (1 - \alpha_g) \phi(\mathbf{x}; \boldsymbol{\mu}_g, \eta_g \boldsymbol{\Sigma}_g)]. \quad (5)$$

Because our contaminated approach contains $2G$ components, i.e., G top-level components, each of which contains two second-level components, the model in (1) shall be considered to contain G clusters, rather than G components, hereafter. Based on this consideration, model (5) can be seen as a special case of the multi-layer mixture of normal distributions of Li (2005) if each of the G clusters at the top level is itself a mixture of two components, with equal means and proportional covariance matrices at the secondary layer.

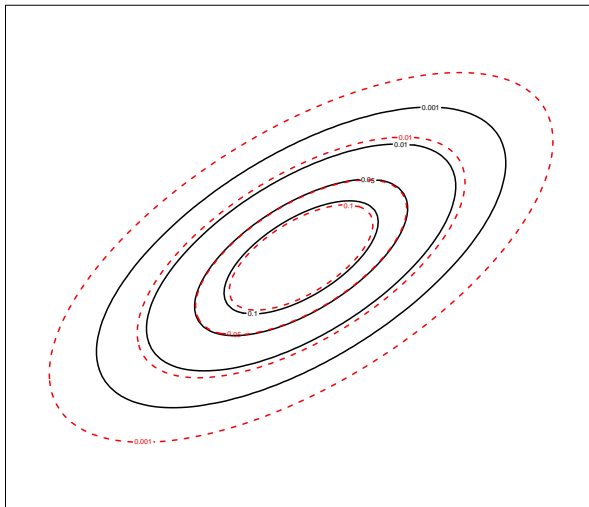


Figure 1: Example of contours illustrating the inflation effect of the constraint that $\eta > 1$. A normal distribution (solid black contours) is compared to a contaminated normal distribution (dashed red contours) with $\alpha = 0.8$ and $\eta = 3$.

2.2. Parsimonious variants of the general model

Because there are $p(p+1)/2$ free parameters for each Σ_g , it is usually necessary to introduce parsimony into the model in (5). Following Banfield and Raftery (1993) and Celeux and Govaert (1995), we consider the eigen-decomposition

$$\Sigma_g = \lambda_g \Gamma_g \Delta_g \Gamma_g', \quad (6)$$

where $\lambda_g = |\Sigma_g|^{1/p}$, Δ_g is the scaled ($|\Delta_g| = 1$) diagonal matrix of the eigenvalues of Σ_g sorted in decreasing order, and Γ_g is a $p \times p$ orthogonal matrix whose columns are the normalized eigenvectors of Σ_g , ordered according to their eigenvalues. Each element in the right-hand side of (6) has a different geometric interpretation: λ_g determines the volume of the g th cluster of the good data only, Δ_g determines the shape of the cluster, and Γ_g determines the orientation of the cluster. Based on (4), the volume of the cluster is given by $\lambda_g [\alpha_g + (1 - \alpha_g) \eta_g]$.

In the fashion of Celeux and Govaert (1995), we impose constraints on the three components of (6) resulting in a family of fourteen parsimonious mixtures of contaminated normal distributions models (Table 1). The last column of Table 1 specifies the scale invariant models of this family.

Family	Model	Volume	Shape	Orientation	Σ_g	# of free parameters in $\Sigma_1, \dots, \Sigma_G$	Scale invariant
Spherical	EII	Equal	Spherical	-	$\lambda \mathbf{I}$	1	No
	VII	Variable	Spherical	-	$\lambda_g \mathbf{I}$	G	No
Diagonal	E EI	Equal	Equal	Axis-Aligned	$\lambda \Delta$	p	Yes
	VEI	Variable	Equal	Axis-Aligned	$\lambda_g \Delta$	$G + p - 1$	Yes
	EVI	Equal	Variable	Axis-Aligned	$\lambda \Delta_g$	$1 + G(p - 1)$	Yes
	VVI	Variable	Variable	Axis-Aligned	$\lambda_g \Delta_g$	Gp	Yes
General	EEE	Equal	Equal	Equal	$\lambda \Gamma \Delta \Gamma'$	$p(p + 1)/2$	Yes
	VEE	Variable	Equal	Equal	$\lambda_g \Gamma \Delta \Gamma'$	$G + p - 1 + p(p - 1)/2$	Yes
	EVE	Equal	Variable	Equal	$\lambda \Gamma \Delta_g \Gamma'$	$1 + G(p - 1) + p(p - 1)/2$	No
	EEV	Equal	Equal	Variable	$\lambda \Gamma_g \Delta \Gamma_g'$	$p + Gp(p - 1)/2$	No
	VVE	Variable	Variable	Equal	$\lambda_g \Gamma_g \Delta_g \Gamma_g'$	$Gp + p(p - 1)/2$	No
	VEV	Variable	Equal	Variable	$\lambda_g \Gamma_g \Delta \Gamma_g'$	$G + p - 1 + Gp(p - 1)/2$	No
	EVV	Equal	Variable	Variable	$\lambda \Gamma_g \Delta_g \Gamma_g'$	$1 + G(p - 1) + Gp(p - 1)/2$	Yes
	VVV	Variable	Variable	Variable	$\lambda_g \Gamma_g \Delta_g \Gamma_g'$	$Gp(p + 1)/2$	Yes

Table 1: Nomenclature, covariance structure, and number of free parameters in $\Sigma_1, \dots, \Sigma_G$ for the models of our family.

2.3. Model-based clustering

The idea of defining clustering in terms of the components of a mixture model goes back at least 60 years (cf. McNicholas, 2016, Section 2.1), and model-based clustering has become increasingly popular since mixture models were first used for clustering (Wolfe, 1965). Consider n independent p -dimensional unlabeled observations $\{\mathbf{x}_i\}_{i=1}^n$ from model (5), and let $\{z_i\}_{i=1}^n$ denote cluster memberships, where $\mathbf{z}_i = (z_{i1}, \dots, z_{iG})'$ and $z_{ig} = 1$ if \mathbf{x}_i belongs to cluster g and $z_{ig} = 0$ otherwise. Using the same notation as before, the model-based clustering likelihood is given by

$$L(\boldsymbol{\psi}) = \prod_{i=1}^n p(\mathbf{x}_i; \boldsymbol{\psi}),$$

and the predicted classifications are given by the maximum *a posteriori* probabilities (MAP). Note that

$$\text{MAP}(\hat{z}_{ig}) = \begin{cases} 1 & \text{if } \max_h \{\hat{z}_{ih}\} \text{ occurs in cluster } g, \\ 0 & \text{otherwise,} \end{cases}$$

where

$$\hat{z}_{ig} = \frac{\hat{\pi}_g f(\mathbf{x}_i; \hat{\boldsymbol{\vartheta}}_g)}{p(\mathbf{x}_i; \hat{\boldsymbol{\psi}})} = \frac{\hat{\pi}_g f(\mathbf{x}_i; \hat{\boldsymbol{\vartheta}}_g)}{\sum_{h=1}^G \hat{\pi}_h f(\mathbf{x}_i; \hat{\boldsymbol{\vartheta}}_h)}$$

is the *a posteriori* expected value of Z_{ig} given \mathbf{x}_i , i.e., the probability that $Z_{ig} = 1$ given \mathbf{x}_i and based on the parameter estimates $\hat{\boldsymbol{\psi}}$.

3. Identifiability

Before outlining parameter estimation for the models in our family, it is important to establish their identifiability. Identifiability is a necessary requirement, *inter alia*, for the usual asymptotic theory to hold for maximum likelihood estimation of the model parameters (cf. Section 4). Before investigating the identifiability of our contaminated mixtures, it is convenient to rewrite the model density as

$$p(\mathbf{x}; \boldsymbol{\psi}) = \sum_{g=1}^G \sum_{h=1}^2 \pi_g \alpha_{gh} \phi(\mathbf{x}; \boldsymbol{\mu}_g, \eta_{gh} \boldsymbol{\Sigma}_g),$$

where, with respect to equation (5), $\alpha_{g1} = \alpha_g$, $\alpha_{g2} = 1 - \alpha_{g1}$, $\eta_{g1} = 1$, and $\eta_{g2} = \eta_g$.

Identifiability of univariate and multivariate finite mixtures of normal distributions has been proved by Teicher (1963) and Yakowitz and Spragins (1968), respectively. As stated by Di Zio et al. (2007), in the absence of any constraint, a mixture of mixtures is not identifiable in general; this is essentially due to the possibility of interchanging component labels between the two levels of the model. In our case, the contaminated normal distribution $f(\mathbf{x}; \boldsymbol{\vartheta}_g)$ in cluster g is elliptical, and sufficient conditions for identifiability of finite mixtures of elliptical distributions are given in Holzmann et al. (2006). However, these conditions will only apply here if we fix α_g and η_g *a priori*. To avoid the requirement to fix parameters in advance, we need to take a different approach to prove identifiability.

In Proposition 1, it will be shown that the most general model in our family (i.e., VVV) is identifiable provided that, given two of the G normal distributions $\phi(\mathbf{x}; \boldsymbol{\mu}_g, \boldsymbol{\Sigma}_g)$ representing the good observations, they have distinct means and/or non-proportional covariance matrices. It is easy to show that the same sufficient condition also holds for the models EVI, VVI, EVE, EEV, VVE, VEV, and EVV. Proposition 2 shows that the VEE model is identifiable provided that, given two of the G normal distributions $\phi(\mathbf{x}; \boldsymbol{\mu}_g, \boldsymbol{\Sigma}_g)$ representing the good observations, they have distinct means. It is straightforward to show that the same sufficient condition also holds for the nested models: EII, VII, EEI, VEI, and EEE.

Proposition 1. *Let*

$$p(\mathbf{x}; \boldsymbol{\psi}) = \sum_{g=1}^G \sum_{h=1}^2 \pi_g \alpha_{gh} \phi(\mathbf{x}; \boldsymbol{\mu}_g, \eta_{gh} \boldsymbol{\Sigma}_g)$$

and

$$p(\mathbf{x}; \tilde{\boldsymbol{\psi}}) = \sum_{s=1}^{\tilde{G}} \sum_{t=1}^2 \tilde{\pi}_s \tilde{\alpha}_{st} \phi(\mathbf{x}; \tilde{\boldsymbol{\mu}}_s, \tilde{\eta}_{st} \tilde{\boldsymbol{\Sigma}}_s)$$

be two different parameterizations of the unconstrained model (i.e., VVV). If $g \neq g_1$ implies

$$\|\boldsymbol{\mu}_g - \boldsymbol{\mu}_{g_1}\|_2^2 + \|\boldsymbol{\Sigma}_g - a\boldsymbol{\Sigma}_{g_1}\|_2^2 \neq 0 \quad (7)$$

for all $a > 0$, where $\|\cdot\|_2$ is the Froebenius norm, then the equality $p(\mathbf{x}; \boldsymbol{\psi}) = p(\mathbf{x}; \tilde{\boldsymbol{\psi}})$ implies that $G = \tilde{G}$ and also implies that there exists a relabelling such that

$$\pi_g = \tilde{\pi}_g, \quad \alpha_{gh} = \tilde{\alpha}_{gh}, \quad \boldsymbol{\mu}_g = \tilde{\boldsymbol{\mu}}_g, \quad \boldsymbol{\Sigma}_g = \tilde{\boldsymbol{\Sigma}}_g, \quad \text{and} \quad \eta_{gh} = \tilde{\eta}_{gh}.$$

Proof. The identifiability of finite mixtures of normal distributions guarantees that $2G = 2\tilde{G}$, i.e., $G = \tilde{G}$, and, for each pair (g, h) , there exists a pair (s, t) such that

$$\pi_g \alpha_{gh} = \tilde{\pi}_s \tilde{\alpha}_{st}, \quad \boldsymbol{\mu}_g = \tilde{\boldsymbol{\mu}}_s, \quad \text{and} \quad \eta_{gh} \boldsymbol{\Sigma}_g = \tilde{\eta}_{st} \tilde{\boldsymbol{\Sigma}}_s; \quad (8)$$

cf. Di Zio et al. (2007). Note that Condition (7), the fact that $\eta_{g2} > \eta_{g1}$ ($\eta_{s2} > \eta_{s1}$), and the positivity of all the weights π_g and α_{gh} (π_s and α_{st}) avoids nonidentifiability due to potential overfitting (a potential problem for identifiability first noted by Crawford, 1994). In particular, the positivity constraint on the weights avoids nonidentifiability due to empty components while the remaining two constraints avoid nonidentifiability due to identical components.

Based on Condition (7), only two of the $2G$ normal distributions — those with corresponding g for the first parameterization (s for the second) — can have the same mean and proportional covariance matrices. Hence, for each pair (g, s) , with $g, s \in \{1, \dots, G\}$, satisfying (8), the problem reduces to comparing the pair

$$\{\{\pi_g \alpha_{g1}, \eta_{g1} \boldsymbol{\Sigma}_g\}, \{\pi_g \alpha_{g2}, \eta_{g2} \boldsymbol{\Sigma}_g\}\} \quad (9)$$

with the pair

$$\left\{ \left\{ \tilde{\pi}_s \tilde{\alpha}_{s1}, \tilde{\eta}_{s1} \tilde{\boldsymbol{\Sigma}}_s \right\}, \left\{ \tilde{\pi}_s \tilde{\alpha}_{s2}, \tilde{\eta}_{s2} \tilde{\boldsymbol{\Sigma}}_s \right\} \right\}. \quad (10)$$

Thanks to the constraint that the inflation parameters η_{g2} and η_{s2} must be greater than one, it is easy to show that $\eta_{g2} = \tilde{\eta}_{s2}$ and $\boldsymbol{\Sigma}_g = \tilde{\boldsymbol{\Sigma}}_s$. In particular, if we compare the first covariance matrix in (9) with the first covariance matrix in (10), and the second covariance matrix in (9) with the second covariance matrix in (10), we obtain

$$\begin{cases} \eta_{g1} \boldsymbol{\Sigma}_g = \tilde{\eta}_{s1} \tilde{\boldsymbol{\Sigma}}_s \\ \eta_{g2} \boldsymbol{\Sigma}_g = \tilde{\eta}_{s2} \tilde{\boldsymbol{\Sigma}}_s \end{cases} \Rightarrow \begin{cases} \eta_{g2} = \tilde{\eta}_{s2} \\ \boldsymbol{\Sigma}_g = \tilde{\boldsymbol{\Sigma}}_s \end{cases}, \quad (11)$$

which is exactly what we need for identifiability. In (11), we have used the fact that, by definition, $\eta_{g1} = \tilde{\eta}_{s1} = 1$. On the contrary, if we consider the remaining possibility to compare the first covariance matrix in (9) with the second covariance matrix in (10), and the second covariance matrix in (9) with the first covariance matrix in (10), we obtain the impossible equation $\eta_{g2} \tilde{\eta}_{s2} = 1$; this equation is impossible because η_{g2} and η_{s2} are both greater than one.

With regard to the mixture weights, we know from (11) that the first element of (9) is related to the first element of (10) and the second element of (9) is related to the second element of (10); accordingly, we have only to compare the corresponding weights. In particular, we obtain

$$\begin{cases} \pi_g \alpha_{g1} = \tilde{\pi}_s \tilde{\alpha}_{s1} \\ \pi_g \alpha_{g2} = \tilde{\pi}_s \tilde{\alpha}_{s2} \end{cases} \Rightarrow \begin{cases} \pi_g \alpha_{g1} = \tilde{\pi}_s \tilde{\alpha}_{s1} \\ \pi_g (1 - \alpha_{g1}) = \tilde{\pi}_s (1 - \tilde{\alpha}_{s1}) \end{cases} \Rightarrow \begin{cases} \pi_g = \tilde{\pi}_s \\ \alpha_{g1} = \tilde{\alpha}_{s1} \end{cases}. \quad (12)$$

Finally, based on (8), (11), and (12), after a suitable relabelling, we obtain

$$\pi_g = \tilde{\pi}_g, \quad \alpha_{gh} = \tilde{\alpha}_{gh}, \quad \boldsymbol{\mu}_g = \tilde{\boldsymbol{\mu}}_g, \quad \lambda_g = \tilde{\lambda}_g, \quad \boldsymbol{\Omega} = \tilde{\boldsymbol{\Omega}}, \quad \text{and} \quad \eta_{gh} = \tilde{\eta}_{gh},$$

with $g \in \{1, \dots, G\}$ and $h \in \{1, 2\}$, and this completes the proof. \square

Proposition 2. *Let*

$$p(\mathbf{x}; \boldsymbol{\psi}) = \sum_{g=1}^G \sum_{h=1}^2 \pi_g \alpha_{gh} \phi(\mathbf{x}; \boldsymbol{\mu}_g, \eta_{gh} \lambda_g \boldsymbol{\Omega})$$

and

$$p(\mathbf{x}; \tilde{\boldsymbol{\psi}}) = \sum_{s=1}^{\tilde{G}} \sum_{t=1}^2 \tilde{\pi}_s \tilde{\alpha}_{st} \phi(\mathbf{x}; \tilde{\boldsymbol{\mu}}_s, \tilde{\eta}_{st} \tilde{\lambda}_s \tilde{\boldsymbol{\Omega}})$$

be two different parameterizations of the VEE model, with $\boldsymbol{\Omega} = \boldsymbol{\Gamma} \boldsymbol{\Delta} \boldsymbol{\Gamma}'$ and $\tilde{\boldsymbol{\Omega}} = \tilde{\boldsymbol{\Gamma}} \tilde{\boldsymbol{\Delta}} \tilde{\boldsymbol{\Gamma}}'$. If $g \neq g_1$ implies

$$\|\boldsymbol{\mu}_g - \boldsymbol{\mu}_{g_1}\|_2^2 \neq 0, \quad (13)$$

then the equality $p(\mathbf{x}; \boldsymbol{\psi}) = p(\mathbf{x}; \tilde{\boldsymbol{\psi}})$ implies that $G = \tilde{G}$ and that there exists a relabelling such that

$$\pi_g = \tilde{\pi}_g, \quad \alpha_{gh} = \tilde{\alpha}_{gh}, \quad \boldsymbol{\mu}_g = \tilde{\boldsymbol{\mu}}_g, \quad \lambda_g = \tilde{\lambda}_g, \quad \boldsymbol{\Omega} = \tilde{\boldsymbol{\Omega}}, \quad \text{and} \quad \eta_{gh} = \tilde{\eta}_{gh}.$$

Proof. Noting that the assumption $|\boldsymbol{\Delta}| = 1$ (and $|\tilde{\boldsymbol{\Delta}}| = 1$) ensures that $\boldsymbol{\Omega} = \tilde{\boldsymbol{\Omega}}$, the proof is almost identical to the proof of Proposition 1. \square

4. Maximum likelihood estimation

4.1. An ECM algorithm

To fit the models of our family, we use the expectation-conditional maximization (ECM) algorithm (Meng and Rubin, 1993). The ECM algorithm is a variant of the classical expectation-maximization (EM) algorithm (Dempster et al., 1977), which is a natural approach for maximum likelihood estimation when data are incomplete. In our case, there are two sources of missing data: one arises from the fact that we do not know the cluster labels $\{\mathbf{z}_i\}_{i=1}^n$ and the other arises from the fact that we do not know whether an observation in group g is good or bad. To denote this second source of missing data, we use $\{\mathbf{v}_i\}_{i=1}^n$, where $\mathbf{v}_i = (v_{i1}, \dots, v_{iG})'$ so that $v_{ig} = 1$ if observation i in group g is good and $v_{ig} = 0$ if observation i in group g is bad. Therefore, the complete-data are given by $\mathcal{S} = \{\mathbf{x}_i, \mathbf{z}_i, \mathbf{v}_i\}_{i=1}^n$, and the complete-data log-likelihood can be written

$$l_c(\boldsymbol{\psi}|\mathcal{S}) = l_{1c}(\boldsymbol{\pi}|\mathcal{S}) + l_{2c}(\boldsymbol{\alpha}|\mathcal{S}) + l_{3c}(\boldsymbol{\theta}|\mathcal{S}), \quad (14)$$

where

$$l_{1c}(\boldsymbol{\pi}|\mathcal{S}) = \sum_{i=1}^n \sum_{g=1}^G z_{ig} \ln \pi_g, \quad l_{2c}(\boldsymbol{\alpha}|\mathcal{S}) = \sum_{i=1}^n \sum_{g=1}^G z_{ig} [v_{ig} \ln \alpha_g + (1 - v_{ig}) \ln (1 - \alpha_g)],$$

$$l_{3c}(\boldsymbol{\theta}|\mathcal{S}) = -\frac{1}{2} \sum_{i=1}^n \sum_{g=1}^G \left\{ z_{ig} \ln |\boldsymbol{\Sigma}_g| + p z_{ig} (1 - v_{ig}) \ln \eta_g + z_{ig} \left(v_{ig} + \frac{1 - v_{ig}}{\eta_g} \right) \delta(\mathbf{x}_i, \boldsymbol{\mu}_g; \boldsymbol{\Sigma}_g) \right\},$$

with $\boldsymbol{\alpha} = (\alpha_1, \dots, \alpha_G)'$ and $\boldsymbol{\theta} = \{\boldsymbol{\mu}_g, \boldsymbol{\Sigma}_g, \eta_g\}_{g=1}^G$. The ECM algorithm iterates between three steps, an E-step and two CM-steps, until convergence. The only difference from the EM algorithm is that each M-step is replaced by two simpler CM-steps. They arise from the partition $\boldsymbol{\psi} = \{\boldsymbol{\psi}_1, \boldsymbol{\psi}_2\}$, where $\boldsymbol{\psi}_1 = \{\pi_g, \alpha_g, \boldsymbol{\mu}_g, \boldsymbol{\Sigma}_g\}_{g=1}^G$ and $\boldsymbol{\psi}_2 = \{\eta_g\}_{g=1}^G$.

4.2. Model VVV

Here, we detail the ECM algorithm for the most general VVV model (5) under no constraint for α_g , i.e., $\alpha_g \in (0, 1)$, $g = 1, \dots, G$.

4.2.1. E-step.

The E-step, on the $(r + 1)$ th iteration of the ECM algorithm, requires the calculation of $Q(\boldsymbol{\psi}|\boldsymbol{\psi}^{(r)})$, the current conditional expectation of $l_c(\boldsymbol{\psi}|\mathcal{S})$. To do this, we need to calculate $E_{\boldsymbol{\psi}^{(r)}}(Z_{ig}|\mathbf{x}_i)$ and $E_{\boldsymbol{\psi}^{(r)}}(V_{ig}|\mathbf{x}_i, \mathbf{z}_i)$, for $i = 1, \dots, n$ and $g = 1, \dots, G$. They are given by

$$E_{\boldsymbol{\psi}^{(r)}}(Z_{ig}|\mathbf{x}_i) = \frac{\pi_g^{(r)} f(\mathbf{x}_i; \boldsymbol{\vartheta}_g^{(r)})}{p(\mathbf{x}_i; \boldsymbol{\psi}^{(r)})} =: z_{ig}^{(r)}$$

and

$$E_{\boldsymbol{\psi}^{(r)}}(V_{ig}|\mathbf{x}_i, \mathbf{z}_i) = \frac{\alpha_g^{(r)} \phi(\mathbf{x}_i; \boldsymbol{\mu}_g^{(r)}, \boldsymbol{\Sigma}_g^{(r)})}{f(\mathbf{x}_i; \boldsymbol{\vartheta}_g^{(r)})} =: v_{ig}^{(r)}, \quad (15)$$

respectively. Then, by substituting z_{ig} with $z_{ig}^{(r)}$ and v_{ig} with $v_{ig}^{(r)}$ in (14), we obtain $Q(\boldsymbol{\psi}|\boldsymbol{\psi}^{(r)})$.

4.2.2. CM-step 1.

The first CM-step on the $(r + 1)$ th iteration of the ECM algorithm requires the calculation of $\boldsymbol{\psi}_1^{(r+1)}$ as the value of $\boldsymbol{\psi}_1$ that maximizes $Q(\boldsymbol{\psi}|\boldsymbol{\psi}^{(r)})$ with $\boldsymbol{\psi}_2$ fixed at $\boldsymbol{\psi}_2^{(r)}$. In particular, we obtain

$$\pi_g^{(r+1)} = \frac{n_g^{(r)}}{n}, \quad \alpha_g^{(r+1)} = \frac{1}{n_g^{(r)}} \sum_{i=1}^n z_{ig}^{(r)} v_{ig}^{(r)},$$

$$\boldsymbol{\mu}_g^{(r+1)} = \frac{1}{s_g^{(r)}} \sum_{i=1}^n z_{ig}^{(r)} \left(v_{ig}^{(r)} + \frac{1 - v_{ig}^{(r)}}{\eta_g^{(r)}} \right) \mathbf{x}_i, \quad (16)$$

$$\boldsymbol{\Sigma}_g^{(r+1)} = \frac{1}{n_g^{(r)}} \mathbf{W}_g^{(r)}, \quad (17)$$

where

$$s_g^{(r)} = \sum_{i=1}^n z_{ig}^{(r)} \left(v_{ig}^{(r)} + \frac{1 - v_{ig}^{(r)}}{\eta_g^{(r)}} \right), \quad \mathbf{W}_g^{(r+1)} = \sum_{i=1}^n z_{ig}^{(r)} \left(v_{ig}^{(r)} + \frac{1 - v_{ig}^{(r)}}{\eta_g^{(r)}} \right) (\mathbf{x}_i - \boldsymbol{\mu}_g^{(r+1)}) (\mathbf{x}_i - \boldsymbol{\mu}_g^{(r+1)})',$$

and $n_g^{(r)} = \sum_{i=1}^n z_{ig}^{(r)}$.

4.2.3. CM-step 2.

The second CM-step, on the $(r + 1)$ th iteration of the ECM algorithm, requires the calculation of $\boldsymbol{\psi}_2^{(r+1)}$ as the value of $\boldsymbol{\psi}_2$ that maximizes $Q(\boldsymbol{\psi}|\boldsymbol{\psi}^{(r)})$ with $\boldsymbol{\psi}_1$ fixed at $\boldsymbol{\psi}_1^{(r+1)}$. In particular, we have to maximize

$$-\frac{p}{2} \sum_{i=1}^n z_{ig}^{(r)} (1 - v_{ig}^{(r)}) \ln \eta_g - \frac{1}{2} \sum_{i=1}^n z_{ig}^{(r)} \frac{1 - v_{ig}^{(r)}}{\eta_g} \delta(\mathbf{x}_i, \boldsymbol{\mu}_g^{(r+1)}; \boldsymbol{\Sigma}_g^{(r+1)}), \quad (18)$$

with respect to η_g , under the constraint $\eta_g > 1$, for $g = 1, \dots, G$. Operationally, the `optimize()` function, in the `stats` package for R, is used to perform a numerical search of the maximum $\eta_g^{(r+1)}$ of (18) over the interval $(1, \eta^*)$, with $\eta^* > 1$. In the analyses in Section 7, we fix $\eta^* = 1000$ to facilitate faster convergence.

4.3. Parsimonious models

The ECM algorithm for the other models of our family changes only with respect to the way the terms of the eigen-decomposition of Σ_g are obtained in the first CM-step. In particular, these updates are analogous to those given by Celeux and Govaert (1995). The only difference is that, on the $(r + 1)$ th iteration of the algorithm, $\mathbf{W}_g^{(r+1)}$ is used instead of the classical scatter matrix

$$\sum_{i=1}^n z_{ig}^{(r)} \left(\mathbf{x}_i - \boldsymbol{\mu}_g^{(r+1)} \right) \left(\mathbf{x}_i - \boldsymbol{\mu}_g^{(r+1)} \right)'$$

5. Further aspects

5.1. Implementation

R source code implementing the ECM algorithm for all of the models of our family, in the form of an R package, is available from CRAN at <https://cran.r-project.org/web/package=ContaminatedMixt> (Punzo et al., 2015). As a basis to implement our code, we used the `mixture` package (Browne and McNicholas, 2015) for R (R Core Team, 2015), which gives a flexible implementation of the EM algorithm for the family of parsimonious mixtures of multivariate normal distributions introduced by Celeux and Govaert (1995), hereafter abbreviated as GPCM family. The `mixture` package differs from the `Rmixmod` package (Biernacki et al., 2008; Lebre et al., 2012) with respect to the algorithm used in the M-step to estimate parameters for the EVE and VVE models. In particular, the `Rmixmod` package adopts the classical FG-algorithm of Flury and Gautschi (1986), while the `mixture` package makes use of majorization-minimization (MM) algorithms (Hunter and Lange, 2000; Browne and McNicholas, 2014).

5.2. Initialization

The choice of the starting values for EM-based algorithms constitutes an important issue (see, e.g., Biernacki et al., 2003, Karlis and Xekalaki, 2003, and Bagnato and Punzo, 2013). For the ECM algorithm described before, two natural strategies are:

1. providing the initial quantities $\mathbf{z}_i^{(0)}$, $\mathbf{v}_i^{(0)}$, and $\eta_g^{(0)}$, $i = 1, \dots, n$ and $g = 1, \dots, G$, to the first CM-step of the first iteration; and
2. selecting an initial value $\boldsymbol{\psi}^{(0)}$ for $\boldsymbol{\psi}$ in order to run the E-step of the first iteration.

By considering the first strategy, we suggest the following technique. Each (G -cluster) model of the GPCM family tends to the corresponding (G -cluster) model of our family when $\alpha_g \rightarrow 1^-$ and $\eta_g \rightarrow 1^+$, $g = 1, \dots, G$. Under these conditions, $v_{ig} \rightarrow 1^-$, $i = 1, \dots, n$ and $g = 1, \dots, G$. Then, the posterior probabilities from the EM algorithm for each model of the GPCM family — obtained with the `gpcm()` function of the `mixture` package — along with the constraints $v_{ig}^{(0)} = v^{(0)}$, with $v^{(0)} \rightarrow 1^-$, and $\eta_g = \eta^{(0)}$, with $\eta^{(0)} \rightarrow 1^+$, $i = 1, \dots, n$, and $g = 1, \dots, G$, can be used to run the first CM-step of the first iteration of our ECM algorithm. From an operational point of view, thanks to the monotonicity property of the ECM algorithm (see, e.g., McLachlan and Krishnan, 2007, p. 28), this also guarantees that the observed-data log-likelihood of a model from our family will be always greater than or equal to the observed-data log-likelihood of the corresponding model of the GPCM family (nested models); this is a fundamental consideration for the use of likelihood-based model selection criteria for choosing between models of our family and of the GPCM family (cf. Böhning and Ruangroj, 2002 and Punzo et al., 2016). In the analyses of Section 7, $v^{(0)} = 0.999$ and $\eta^{(0)} = 1.001$.

5.3. Convergence criterion

The Aitken acceleration (Aitken, 1926) is used to estimate the asymptotic maximum of the log-likelihood at each iteration of the ECM algorithm. Based on this estimate, we can decide whether or not the algorithm has reached convergence, i.e., whether or not the log-likelihood is sufficiently close to its estimated asymptotic value. The Aitken acceleration at iteration $r + 1$ is given by

$$a^{(r+1)} = \frac{l^{(r+2)} - l^{(r+1)}}{l^{(r+1)} - l^{(r)}},$$

where $l^{(r)}$ is the observed-data log-likelihood value from iteration r . Then, the asymptotic estimate of the log-likelihood at iteration $r + 2$ is given by

$$l_{\infty}^{(r+2)} = l^{(r+1)} + \frac{1}{1 - a^{(r+1)}} \left(l^{(r+2)} - l^{(r+1)} \right);$$

cf. Böhning et al. (1994). The ECM algorithm can be considered to have converged when $l_{\infty}^{(r+2)} - l^{(r+1)} < \epsilon$, with $\epsilon > 0$, provided that this difference is positive (McNicholas et al., 2010). In our analyses, we use $\epsilon = 0.0001$.

5.4. Local maxima and degeneracy of the likelihood

In the case of normal mixtures, it is well-known that the likelihood function: (1) presents spurious local maxima and (2) is unbounded. It tends to infinity when one of the cluster means coincides with a sample observation and the corresponding covariance matrix tends to be singular (cf. Biernacki, 2004). The behaviour of the EM algorithm near a degenerate solution has been studied by Biernacki and Chrétien (2003), Ingrassia (2004), and Ingrassia and Rocci (2007, 2011), who tackle the problem by constraining the value of the smallest eigenvalue of the cluster covariance matrices (see also Hathaway, 1986, for the univariate case). Recently, Browne et al. (2013) consider constraining the smallest eigenvalue, the largest eigenvalue, and both the smallest and largest eigenvalues for a subset of models of the GPCM family. However, all these approaches require an *a priori* choice of the constraints they are based on and no rule of thumb is given to assist this choice. Because further study of the best threshold values for these techniques is beyond the scope of this work, we avoid considering “preventive” approaches in the implementation of the ECM algorithm.

5.5. Some notes on robustness

Based on (16), $\boldsymbol{\mu}_g^{(r+1)}$ is a weighted mean of the \boldsymbol{x}_i values, with weights depending on

$$v_{ig}^{(r)} + \frac{1 - v_{ig}^{(r)}}{\eta_g^{(r)}}. \quad (19)$$

Consider the update for $v_{ig}^{(r)}$, given in (15), as a function of the squared Mahalanobis distance δ , i.e.,

$$h(\delta; \alpha_g, \eta_g) = \frac{\alpha_g \exp\left(-\frac{\delta}{2}\right)}{\alpha_g \exp\left(-\frac{\delta}{2}\right) + \frac{(1-\alpha_g)}{\sqrt{\eta_g}} \exp\left(-\frac{\delta}{2\eta_g}\right)} = \frac{1}{1 + \frac{(1-\alpha_g)}{\alpha_g} \frac{1}{\sqrt{\eta_g}} \exp\left[\frac{\delta}{2}\left(1 - \frac{1}{\eta_g}\right)\right]}, \quad (20)$$

with $\delta \geq 0$. Due to the constraint $\eta_g > 1$, from the last expression of (20) it is straightforward to realize that $h(\delta; \alpha_g, \eta_g)$ is a decreasing function of δ . Based on (20), (19) can be written

$$w(\delta; \alpha_g, \eta_g) = h(\delta; \alpha_g, \eta_g) + \frac{1 - h(\delta; \alpha_g, \eta_g)}{\eta_g} = \frac{1}{\eta_g} [1 + (\eta_g - 1) h(\delta; \alpha_g, \eta_g)]. \quad (21)$$

From the last expression of (21), $w(\delta; \alpha_g, \eta_g)$ is an increasing function of $h(\delta; \alpha_g, \eta_g)$; this also means that $w(\delta; \alpha_g, \eta_g)$ is a decreasing function of δ . Therefore, the weights in (19) reduce the impact of bad points in the estimation of the means $\boldsymbol{\mu}_g$, thereby providing robust estimates of these means. In addition, from (17), the larger δ values also have smaller effect on $\boldsymbol{\Sigma}_g$, $g = 1, \dots, G$, due to the weights in (19). For a discussion on down-weighting for the contaminated normal distribution, see also Little (1988).

5.6. Automatic detection of bad points

For a model belonging to our family, the classification of an observation \mathbf{x}_i means:

Step 1. determine its cluster of membership;

Step 2. establish whether it is a good or a bad observation in that cluster.

Let $\widehat{\mathbf{z}}_i$ and $\widehat{\mathbf{v}}_i$ denote, respectively, the expected values of \mathbf{z}_i and \mathbf{v}_i arising from the ECM algorithm, i.e., \widehat{z}_{ig} is the value of $z_{ig}^{(r)}$ at convergence and \widehat{v}_{ig} is the value of $v_{ig}^{(r)}$ at convergence. To evaluate the cluster membership of \mathbf{x}_i , we use the MAP classification, i.e., $\text{MAP}(\widehat{\mathbf{z}}_{ig})$. We then consider \widehat{v}_{ih} , where h is selected such that $\text{MAP}(\widehat{z}_{ih}) = 1$, and \mathbf{x}_i is considered good if $\widehat{v}_{ih} > 0.5$ and \mathbf{x}_i is considered bad otherwise. The resulting information can be used to eliminate the bad points, if such an outcome is desired (Berkane and Bentler, 1988). The remaining data may then be treated as effectively being distributed according to a mixture of normal distributions, and the clustering results can be reported as usual. Finally, note that a *a posteriori* procedure (i.e., a procedure taking place once the model is fitted) to detect bad points with the mixture of multivariate t distributions is illustrated by McLachlan and Peel (2000, p. 232). Such a procedure relies on a χ^2 -approximation, with p degrees of freedom, of the squared Mahalanobis distances $\delta(\mathbf{x}_i, \boldsymbol{\mu}_g; \boldsymbol{\Sigma}_g)$, $i = 1, \dots, n$, after the MAP classification of each observation \mathbf{x}_i to one of the G groups, and it requires a subjective choice of a percentile of the χ^2 distribution in order for the observation to be classified as good or bad; such a procedure will be applied, for comparison's sake, in the analyses of Sections 6 and 7 by choosing the 95th percentile. On the contrary, the approach proposed herein is natural, in that it simultaneously identifies bad points and down-weights their impact on estimation of the mean (as well as on estimation of the covariance matrix; cf. Section 5.5), makes no additional distributional assumptions, and is not based on subjective choices.

5.7. Constraints for detection of bad points

When our models are used for detection of bad points in each group, $(1 - \alpha_g)$ represents the proportion of bad points and η_g denotes the degree of contamination. Then, for the former parameter, one could require that in the g th group, $g = 1, \dots, G$, the proportion of good data is at least equal to a pre-determined value α_g^* . In this case, the `optimize()` function is also used for a numerical search of the maximum $\alpha_g^{(r+1)}$, over the interval $(\alpha_g^*, 1)$, of the function

$$\sum_{i=1}^n z_{ig}^{(r)} \left[v_{ig}^{(r)} \ln \alpha_g + (1 - v_{ig}^{(r)}) \ln (1 - \alpha_g) \right].$$

In the analyses herein (Section 7), we use this approach to update α_g and, as emphasized in Section 2.1, we take $\alpha_g^* = 0.5$, for $g = 1, \dots, G$. Note that it is also possible to fix α_g and/or η_g *a priori*.

5.8. Model selection

The models from our family, in addition to $\boldsymbol{\psi}$, are also characterized by the particular covariance structure and by the number of clusters G . Thus far, these quantities have been treated as *a priori* fixed; nevertheless, for practical purposes, model selection is usually required. One way (the usual way) to perform model selection is via computation of a convenient (likelihood-based) model selection criterion across all fourteen models and over a reasonable range of values for G , and then choosing the model associated with the best value of the adopted criterion (for the alternative use of likelihood-ratio tests to select either the parsimonious model or the number of components for a normal mixture, see Lo et al., 2001, Lo, 2005, 2008, and Punzo et al., 2016). Based on the simulation study performed by Li (2005) for the multi-layer mixture of normal distributions, in the data analyses of Section 7 we will adopt the Bayesian information criterion (Schwarz, 1978), i.e.,

$$\text{BIC} = -2l(\widehat{\boldsymbol{\psi}}) + m \ln n,$$

where m is the overall number of free parameters in the model. Note that, Bayes factors can be used to compare models that are not nested, and the BIC approximation thereto holds when models are not nested (cf. Raftery, 1995).

6. Simulation study: Comparison between mixtures that handle mild outliers

6.1. Overview

In this section, we investigate the behaviour of the proposed model (for simplicity, in its unconstrained version VVV) through a large-scale simulation study performed using R (R Core Team, 2015). We further provide a comparison with the unconstrained variants of the mixture models handling mild outliers and discussed in Section 1. A general feedback on advantages and drawbacks of each model is also given. We compare:

1. mixture of normal distributions (abbreviated by NM = normal mixture). The `gpcm()` function of the `mixture` package (Browne and McNicholas, 2015) for R is used to fit the unconstrained normal mixture (corresponding to the VVV model based on the nomenclature of the `mixture` package). The `gpcm()` function implements the EM algorithm.
2. mixture of t distributions ($tM = t$ mixture; Andrews and McNicholas, 2012). The `teigen()` function of the `teigen` package (Andrews et al., 2015) for R is used to fit the unconstrained t mixture (corresponding to the UUUU model with respect to the nomenclature of the `teigen` package). The `teigen()` function implements the ECM algorithm described, for example, in (Andrews et al., 2015). Degrees of freedom are estimated and they are allowed to vary across groups.
3. mixture of contaminated normal distributions (CNM = contaminated normal mixture). The `CNmixt()` function of the `ContaminatedMixt` package (Punzo et al., 2015) for R is used to fit the unconstrained contaminated normal mixture (corresponding to the VVV model with respect to the nomenclature of the `ContaminatedMixt` package). The `CNmixt()` function implements the ECM algorithm described in Section 4.
4. mixture of mixtures of a normal and a uniform distribution (NUM = normal-uniform mixture; Browne et al., 2012). A specific R code, implementing the generalized-EM (GEM) algorithm described in Browne et al. (2012), is used to fit the unconstrained normal-uniform mixture. No constraint is imposed on the component uniform distributions (corresponding to model IV with respect to the nomenclature of Browne et al., 2012).
5. mixture of normal distributions plus a uniform component (NCM = noise component mixture; Banfield and Raftery, 1993). The `Mclust()` function of the `mclust` package (Fraley et al., 2012, 2015) for R is used to fit the unconstrained noise component mixture (corresponding to the VVV model with respect to the nomenclature of the `mclust` package). The `Mclust()` function implements the EM algorithm.

To generate the data, we consider the following five data generation processes with $p = 2$ dimensions and $G = 2$ clusters:

- a) NM;
- b) tM with $\nu_1 = 4$ and $\nu_2 = 10$ degrees of freedom;
- c) CNM with $\alpha_1 = 0.9$, $\alpha_2 = 0.8$, $\eta_1 = 20$, and $\eta_2 = 30$;
- d) NM with 1% of points randomly substituted by high atypical points with coordinates $(0, x_{i2}^*)$, where x_{i2}^* is generated from a uniform distribution over the interval $(10, 15)$.
- e) NM with 5% of points randomly substituted by noise points generated from a uniform distribution over the interval $(-10, 10)$ on each dimension.

All of these data generation processes share the following common parameters

$$\pi_1 = 0.3, \quad \boldsymbol{\mu}_2 = \begin{pmatrix} 0 \\ 3 \end{pmatrix}, \quad \boldsymbol{\Sigma}_1 = \begin{pmatrix} 1 & -0.5 \\ -0.5 & 1 \end{pmatrix}, \quad \text{and} \quad \boldsymbol{\Sigma}_2 = \begin{pmatrix} 1 & 0.5 \\ 0.5 & 1 \end{pmatrix}.$$

As concerns the mean in the first group, two alternatives are considered in order to reproduce two different degrees of overlap between clusters: $\boldsymbol{\mu}_1 = (0, -3)'$ in the “far” case, and $\boldsymbol{\mu}_1 = (0, -1)'$ in the “close” case. The five scenarios above cover different situations which may arise dealing with real-world data: no bad points for scenario *a*), heavy-tails cluster distributions for scenarios *b*) and *c*), and two different types of bad points for scenarios *d*) and *e*). Under each scenario, we simulate 1,000 samples considering the number of analyzed units n (100, 200, and 500), as well as the degree of overlap (“far” and “close”), as experimental factors. This yields a total of 30,000 generated data sets. On each generated data set, the five competing models are directly run with $G = 2$. As concerns the initialization strategy of the EM-based algorithms for the first four models (NM, *t*M, CNM, and NUM), the partition provided by the *k*-means method, as implemented by the `kmeans()` function, with default arguments, of the `stats` package for R, is considered. As concerns the NCM, an initial guess of the noise observations must be supplied via the `noise` component of the `initialization` argument in `Mclust()`. Nearest neighbor based clutter/noise detection proposed by Byers and Raftery (1998) is applied to identify an initial set of noise points. The latter is implemented in the `NNclean()` function in R’s `prabclus` package (Hennig and Hausdorf, 2015). Agglomerative hierarchical clustering based on ML criteria for normal mixtures proposed by Banfield and Raftery (1993) is then used for finding initial normal clusters in the non-noise data. This is implemented in the `hc()` function of R’s `mclust` package.

Before presenting the obtained results, we want to underline that the average elapsed time (in seconds over the 30,000 replications) to fit a single CNM is 0.692 seconds. This information is useful to have an idea of the computational burden required by our ECM algorithm. Computation is performed on a Windows 8.1 PC, with Intel i7 3.50GHz CPU, 16.0 GB RAM, using R 32 bit, and the elapsed time is computed via the `proc.time()` function of the `base` package.

6.2. Parameter estimation

For comparison’s sake, we report the bias (BIAS) and the standard deviation (STD) of the estimates for the mixture weight π_1 , the univariate means μ_{11} and μ_{21} (elements of $\boldsymbol{\mu}_1$), and the univariate means μ_{12} and μ_{22} (elements of $\boldsymbol{\mu}_2$). Before to illustrate the obtained results, it is important to underline that under mixture models there are well known label switching issues (see, e.g., Celeux et al., 2000, Stephens, 2000, and Yao, 2012) when evaluating properties of the estimators of the parameters using simulation studies. There are no generally accepted labeling methods. In our simulation study, as in Bai et al. (2012) and Yao et al. (2014), we choose the labels by minimizing the distance to the true parameter values.

Table 2 reports the results under scenario *a*), that is when there are no bad points. Here, as expected, NMs, *t*Ms, and CNMs perform comparably because, in this situation, the *t*M and the CNM tend to the NM. NCMs work well too, apart from the estimation of the mixture weights, while NUMs provide the worst results. Finally, regardless of both the considered model and the parameter of interest, the BIAS and the STD values improve with the increase of n and they are better under the “far” case, as expected.

Table 3 and 4 report the results under scenarios *b*) and *c*), respectively. Here, the robust approaches (*t*M, CNM, NUM, and NCM) are better than the traditional NM. As expected, the best performer is the *t*M under scenario *b*) and the CNM under scenario *c*). These models are the best two under these scenarios; their comparable behavior agrees with the simulation results of Little (1988) about the single *t* and the contaminated normal distributions. NUMs and NCMs work slightly better than NMs but far worse from *t*Ms and CNMs (see, e.g., the STD values, in the case $n = 100$, in Table 4).

Table 5 reports the results under scenario *d*), that is when there is the 1% of bad points with a specific location in the space. By focusing on the STD values, *t*Ms and CNMs perform comparably, with a slightly better performance for CNMs when the sample size is small ($n = 100$). Surprisingly, NUM and NCM perform worse than NM (refer, e.g., to the case $n = 100$).

Finally, Table 6 reports the results under scenario *e*), that is when there is the 5% of bad points on the background of the bulk of the data. For the way the outliers are added, the NCM should be the best performer; instead, the best performance is for the CNM, regardless of both the overlap and the sample size.

	n		NM		tM		CNM		NUM		NCM	
			BIAS	STD	BIAS	STD	BIAS	STD	BIAS	STD	BIAS	STD
Far	100	$\pi_1 = 0.3$	0.030	0.095	0.026	0.089	0.014	0.059	0.019	0.075	0.103	0.303
		$\mu_{11} = 0$	-0.014	0.419	0.004	0.247	0.005	0.246	0.009	0.365	0.026	0.455
		$\mu_{21} = -3$	-0.029	0.621	0.043	0.516	-0.003	0.235	0.078	0.548	0.191	1.007
		$\mu_{12} = 0$	-0.070	0.941	-0.012	0.870	0.004	0.150	0.021	0.175	0.032	1.637
		$\mu_{22} = 3$	0.083	0.563	-0.020	0.344	-0.008	0.165	0.023	0.168	-0.064	1.220
	200	$\pi_1 = 0.3$	0.034	0.086	0.029	0.084	0.012	0.036	0.010	0.059	0.086	0.306
		$\mu_{11} = 0$	-0.058	0.260	-0.004	0.151	-0.005	0.141	-0.011	0.282	-0.010	0.218
		$\mu_{21} = -3$	0.108	0.619	0.058	0.555	-0.007	0.149	0.137	0.497	0.144	0.838
		$\mu_{12} = 0$	-0.059	0.856	-0.073	0.911	0.005	0.097	0.029	0.113	-0.044	1.197
		$\mu_{22} = 3$	0.076	0.363	-0.009	0.347	0.001	0.094	0.033	0.110	0.003	0.838
	500	$\pi_1 = 0.3$	0.045	0.079	0.028	0.057	0.010	0.024	0.008	0.057	0.096	0.305
		$\mu_{11} = 0$	-0.040	0.172	0.004	0.092	0.008	0.086	-0.005	0.239	0.002	0.085
$\mu_{21} = -3$		0.353	0.648	0.035	0.365	-0.004	0.089	0.250	0.444	0.025	0.334	
$\mu_{12} = 0$		-0.021	0.882	-0.021	0.592	0.001	0.055	0.034	0.070	-0.037	0.525	
	$\mu_{22} = 3$	0.045	0.449	-0.001	0.188	0.001	0.054	0.046	0.069	-0.012	0.441	
Close	100	$\pi_1 = 0.3$	0.141	0.241	0.051	0.120	0.032	0.107	0.094	0.116	0.033	0.304
		$\mu_{11} = 0$	-0.015	0.576	0.026	0.314	0.019	0.361	-0.047	0.423	0.031	0.390
		$\mu_{21} = -1$	0.577	1.212	0.100	0.582	0.047	0.561	0.660	0.794	0.530	1.199
		$\mu_{12} = 0$	-0.055	1.658	-0.031	1.079	0.008	0.522	0.085	0.334	-0.002	2.072
		$\mu_{22} = 3$	-0.462	1.919	-0.076	0.796	-0.089	0.703	0.013	0.458	-0.338	2.204
	200	$\pi_1 = 0.3$	0.111	0.172	0.040	0.092	0.016	0.044	0.102	0.090	0.055	0.308
		$\mu_{11} = 0$	-0.046	0.374	0.007	0.170	0.009	0.187	-0.112	0.247	-0.007	0.166
		$\mu_{21} = -1$	0.669	0.771	0.074	0.416	0.007	0.193	0.736	0.607	0.279	0.839
		$\mu_{12} = 0$	-0.112	1.315	0.022	0.908	0.005	0.104	0.088	0.216	-0.100	1.777
		$\mu_{22} = 3$	-0.162	1.111	-0.044	0.596	-0.007	0.133	0.078	0.388	-0.195	1.667
	500	$\pi_1 = 0.3$	0.117	0.093	0.047	0.091	0.015	0.025	0.125	0.071	0.089	0.306
		$\mu_{11} = 0$	-0.045	0.202	-0.008	0.101	-0.001	0.098	-0.161	0.154	-0.012	0.097
$\mu_{21} = -1$		0.800	0.400	0.083	0.411	-0.002	0.107	0.884	0.488	0.110	0.528	
$\mu_{12} = 0$		-0.056	0.891	-0.106	0.980	-0.000	0.060	0.115	0.100	-0.029	1.105	
	$\mu_{22} = 3$	-0.011	0.589	-0.014	0.532	-0.005	0.067	0.146	0.137	-0.152	1.367	

Table 6: Scenario *e*): Simulation results on 1,000 replications.

6.3. Classification performance

Table 7 summarizes the obtained average misclassification rates. Misclassification rates are computed

	n	NM		tM		CNM		NUM		NCM	
		Far	Close	Far	Close	Far	Close	Far	Close	Far	Close
Scenario <i>a</i>)	100	0.002	0.025	0.002	0.025	0.002	0.025	0.086	0.078	0.002	0.038
	200	0.002	0.023	0.002	0.023	0.002	0.023	0.045	0.054	0.001	0.023
	500	0.001	0.021	0.001	0.021	0.001	0.021	0.018	0.037	0.001	0.021
Scenario <i>b</i>)	100	0.018	0.071	0.021	0.068	0.020	0.067	0.043	0.089	0.008	0.059
	200	0.021	0.075	0.023	0.071	0.023	0.072	0.027	0.085	0.008	0.072
	500	0.022	0.080	0.024	0.084	0.024	0.085	0.024	0.099	0.012	0.083
Scenario <i>c</i>)	100	0.091	0.240	0.036	0.069	0.035	0.067	0.102	0.195	0.059	0.118
	200	0.090	0.273	0.034	0.061	0.033	0.060	0.099	0.205	0.036	0.073
	500	0.086	0.293	0.033	0.058	0.030	0.054	0.095	0.213	0.022	0.051
Scenario <i>d</i>)	100	0.005	0.040	0.002	0.026	0.002	0.026	0.057	0.070	0.004	0.043
	200	0.005	0.055	0.002	0.025	0.002	0.023	0.021	0.050	0.008	0.048
	500	0.004	0.061	0.002	0.024	0.001	0.022	0.011	0.039	0.003	0.028
Scenario <i>e</i>)	100	0.006	0.077	0.006	0.033	0.003	0.036	0.024	0.073	0.023	0.090
	200	0.007	0.066	0.005	0.028	0.002	0.025	0.025	0.076	0.012	0.051
	500	0.011	0.050	0.004	0.028	0.001	0.022	0.037	0.080	0.003	0.031

Table 7: Average misclassification rates. Values refer to averages across 1,000 replications.

via the `classError()` function of the `mclust` package for R (Fraley et al., 2012). Under scenarios *d*) and *e*), misclassification rates are computed only with respect to the true good observations; for the NCM only, under all of the considered scenarios, the computation of the misclassification rates is further restricted to the observations which are not assigned, via the MAP operator, to the noise component of the model. Under scenario *a*), in the far case, NM, tM , CNM, and NCM show similar misclassification rates, while misclassification rates from NUM are greater. In the close case, NM, tM , CNM, and NCM provide

analogous results when the sample size is 200 or 500, while NCM gives a slightly greater misclassification rate (0.038) when the sample size is 100. Regardless of the considered sample size, NUM has the worst performance. Under scenario *b*), in the far case, NM, *t*M, and CNM show similar misclassification rates. As concerns the remaining models, NCM has the best performance while NUM the worst. However, the best performance for NCM could be related to the fact that misclassification rates are computed only over the observations classified as good by the model; this means that “problematic” observations in terms of classification (i.e., observations having a similar probability to belong to the two clusters) could be removed from this computation because assigned to the noise component. In the close case, NM, *t*M, CNM, and NCM provide analogous results when the sample size is 200 or 500, while NCM gives a slightly lower misclassification rate (0.059) when the sample size is 100. Regardless of the considered sample size, NUM has the worst performance. Under scenario *c*), regardless of both the overlap between clusters and the sample size, the lowest misclassification rates are obtained (apart from the case $n = 500$) for CNM, followed by *t*M which provides similar results. NUM provides the worst results in the far case, while NM gives the worst misclassification rates in the close case. Under scenarios *d*) and *e*), CNM provides almost always the best results, followed by *t*M. It is interesting to note how CNM works better than NCM under scenarios *e*), which should be the best scenario for NCM. Also in this case, NUM does not provide good results, especially for the far case if compared to the competing models.

6.4. Outlier detection

We now compare the performance of *t*Ms, CNMs, NUMs, and NCMs in detecting outliers. While the MAP operator is adopted to detect outliers for CNMs (cf. Section 5.6), NUMs, and NCMs, for *t*Ms the *a posteriori* procedure illustrated by McLachlan and Peel (2000, p. 232), and summarized at the end of Section 5.6, is considered (with the 95th percentile).

For the purpose of evaluation of the performance of the competing models in detecting outliers, we report the true positive rate (TPR), measuring the proportion of bad points that are correctly identified as bad points, and the false positive rate (FPR), corresponding to the proportion of good points incorrectly classified as bad points. Table 8 reports these measures for scenarios *d*) and *e*). Under scenario *d*), *t*Ms and CNMs show the highest (almost optimal) TPRs, but CNM gives lower (almost optimal) FPRs. The remaining approaches are outperformed by the CNM both in terms of TPRs and FPRs. Under scenario *e*), *t*M gives the highest TPRs. However, this is counterbalanced by higher FPRs. In other words, with the selected percentile, the detection rule for *t*M tends to declare more observations as outliers, but these detected outliers are sometimes not true outliers. If the aim is to remove from the sample the detected outliers, the practical consequence of these results is that, if we use the detection rule from *t*Ms (with the classical percentile we considered), then we are induced to also remove some good observations with a consequent loss of information. Apart from this consideration, the detection rule from *t*Ms needs the specification of a percentile and the simulation results we report show how this choice is not so obvious. On the contrary, the detection rule for CNM provides almost optimal results in terms of FPRs, being their values always close to zero. The fact that the TPRs do not approach at one is not necessarily an error: the way the outliers are inserted into the data makes possible that some of them will have values related to good points and, as such, these points will be detected as good points by our model. Apart from this consideration, the detection rule from *t*-based models needs the specification of a percentile and the simulation results we report show how this choice is not so obvious. With respect to the remaining approaches, regardless of the considered scenario, NCM works better than NUM but worse than *t*M and CNM.

7. Data analyses

In this section, we will evaluate the performance of the 14 parsimonious CNM models on artificial and real data sets. Particular attention will be devoted to the problem of detecting bad points. A comparison with parsimonious families of NMs, *t*Ms, NUMs, and NCMs, will be also provided. These families are implemented by functions and packages already discussed in Section 6. All the EM-based algorithms

	Overlap	n	tM		CNM		NUM		NCM	
			TPR	FPR	TPR	FPR	TPR	FPR	TPR	FPR
Scenario d)	Far	100	1.000	0.070	1.000	0.001	0.976	0.124	0.966	0.096
		200	1.000	0.077	1.000	0.001	0.977	0.042	0.995	0.049
		500	1.000	0.079	1.000	0.000	0.971	0.018	1.000	0.006
	Close	100	0.995	0.059	0.995	0.002	0.970	0.098	0.967	0.111
		200	1.000	0.068	1.000	0.002	0.971	0.030	0.991	0.038
		500	1.000	0.070	1.000	0.001	0.977	0.007	1.000	0.005
Scenario e)	Far	100	0.912	0.077	0.829	0.010	0.695	0.045	0.826	0.048
		200	0.920	0.074	0.833	0.006	0.626	0.042	0.824	0.011
		500	0.923	0.069	0.839	0.002	0.589	0.054	0.834	0.002
	Close	100	0.908	0.068	0.804	0.012	0.694	0.030	0.805	0.027
		200	0.916	0.062	0.854	0.006	0.697	0.014	0.828	0.002
		500	0.920	0.055	0.859	0.002	0.694	0.007	0.847	0.001

Table 8: Values of TPRs and FPRs; they refers to rates across 1,000 replications.

used to fit these models are initialized as explained in Section 6. As concerns the family of parsimonious NUMs and NCMs, based on the R functions used, only a subset of 10 of the 14 parsimonious structures in Table 1 can be implemented; they are: EII, VII, EEI, VEI, EVI, VVI, EEE, EEV, VEV, and VVV.

7.1. Artificial data with uniform noise

In this first analysis, a sample of $n = 180$ simulated bivariate points is generated from an EEE-NM model with $G = 2$ clusters of equal size ($n_1 = n_2 = 90$). Twenty noise points are also added from a uniform distribution over the range -10 to 10 on each variate; hence, the generated data can be meant as arising from an EEE-NCM with $G = 2$ clusters. Note that when a point from this uniform distribution effectively falls inside a cluster, which seems to happen five times (see Figure 2), we would expect it to be classified as belonging to the associated cluster.

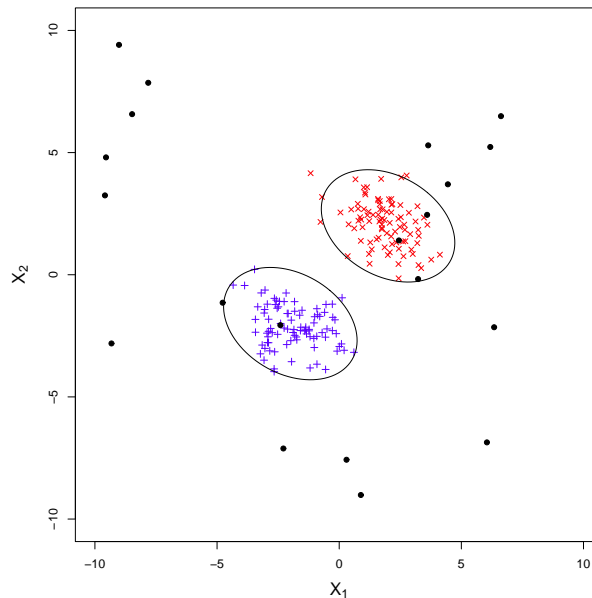


Figure 2: Simulated data from Section 7.1: Scatterplot where uniform noise points are denoted by •.

The competing models are run for $G \in \{1, 2, 3\}$. The corresponding BIC values are reported in Figure 3. From Figure 3(a), the NMs with $G = 3$ clusters have the lowest BIC values. For tM s and CNMs, $G = 2$ and $G = 3$ clusters provide lower BIC values than $G = 1$. For NUMs, 6 of the parsimonious

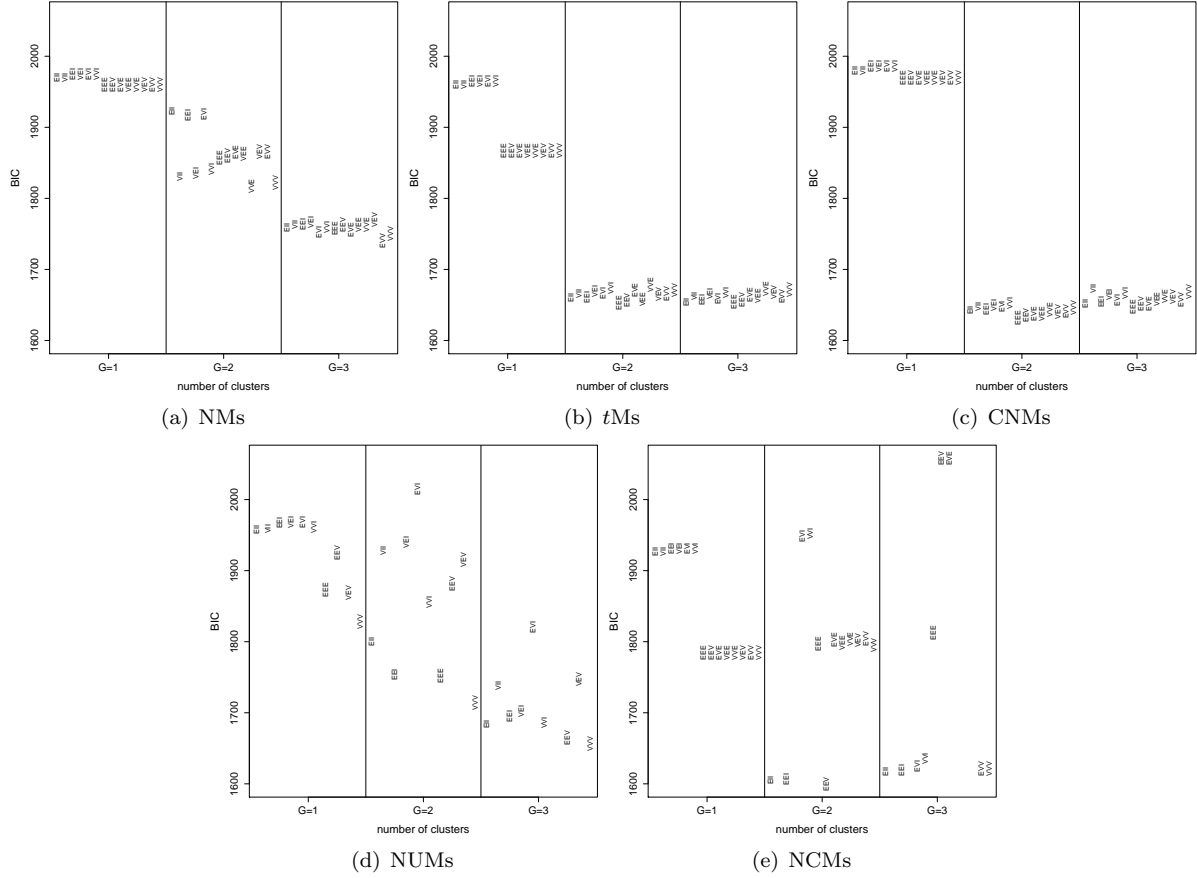


Figure 3: Simulated data from Section 7.1: BIC values for the fitted models.

models with $G = 3$ (VVV, EEV, EII, VVI, EEI, and VEI) have the lowest BIC values. Finally, for NCMs, the best 3 models in terms of BIC have $G = 2$ clusters and covariance structures EEV, EEI, and EII.

For each considered family, the best models according to the BIC are graphically represented in Figure 4; for the selected tM , CNM, NUM, and NCM, detected outliers are denoted by black bullets. For NMs, the best model according to the BIC has $G = 3$ clusters with an EVV covariance structure (Figure 4(a)). We can note how the additional third cluster is attempting to model part of the background noise; however, the remaining part of the noise is erroneously assigned to the other clusters and this contribute to affect the detection of the underlying EEE structure. For tMs and CNMs, the best model according to the BIC is the true one, with corresponding clustering represented in Figure 4(b) and Figure 4(c), respectively. However, in conformity with the simulation results of Section 6.4, the detection rule for tMs , based on the 95th percentile, tends to declare more observations as outliers, but these detected outliers are often not true outliers. The CNM in Figure 4(c) compares very well with the true model (Figure 2), recognizing 15 out of 20 noise observations; as said before, each of the 5 outliers that it does not recognize falls within one of the two clusters (cf. Figure 2). For NUMs, the best model according to the BIC has $G = 3$ clusters with a VVV covariance structure. Amongst the detected 7 outliers, there are 6 true outliers and one point, of the cluster on the left, erroneously detected as outlier (compare Figure 4(d) with Figure 2). Moreover, the third cluster models the part on the right of the background noise. For NCMs, the best model according to the BIC has the correct number of clusters ($G = 2$) but an EEV covariance structure. Apart from the erroneously identified covariance structure, outliers are detected as for CNMs.

Finally, Table 9 reports the number of misclassified observations for each of the best models according

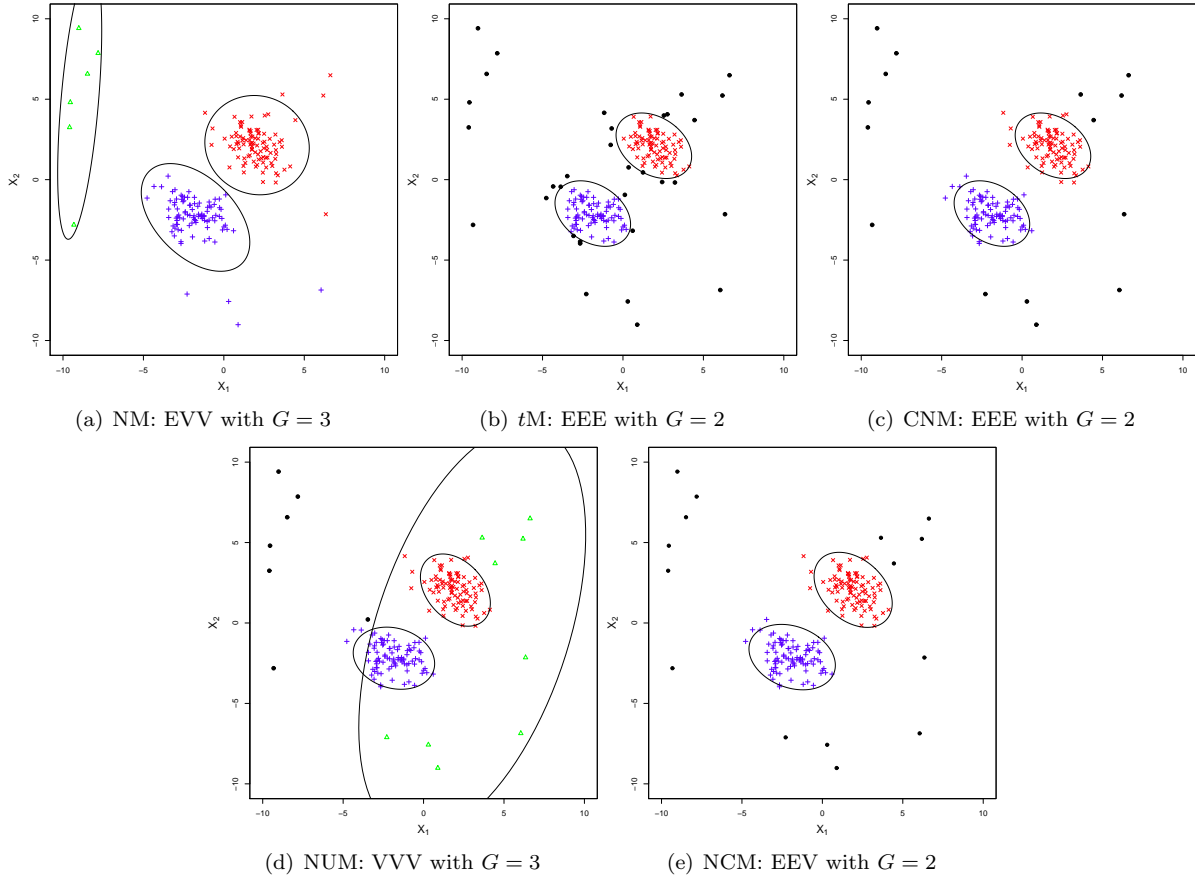


Figure 4: Simulated data from Section 7.1: scatterplots illustrating the best models, according to the BIC, for each considered family. Bullets denote detected bad points.

to the BIC. This number is computed by considering the true classification of the points in: cluster 1, cluster 2, and noise. We can note how the best performers are the CNM and the NCM, with only 5 misclassified observations corresponding to the 5 noisy points falling into the clusters (compare Figure 4(c) and Figure 4(e) with Figure 2).

Model	G	Covariance structure	# of misclassified observations
NM	3	EVV	14
tM	2	EEE	19
CNM	2	EEE	5
NUM	3	VVV	12
NCM	2	EEV	5

Table 9: Simulated data from Section 7.1: number of misclassified observations for the best models according to the BIC.

7.2. Sensitivity study based on the blue crabs data

As a second analysis, a sensitivity study, based on the very popular crabs data set of Campbell and Mahon (1974), is here described to compare how a single bad point affects the behaviour of the competing models. Attention is focused on the sample of $n = 100$ blue crabs of the genus *Leptograpsus*, of which there are 50 males and 50 females (Figure 5). For each specimen, we consider two measurements (in millimeters), namely the rear width (RW) and the length along the midline of the carapace (CL). In the fashion of

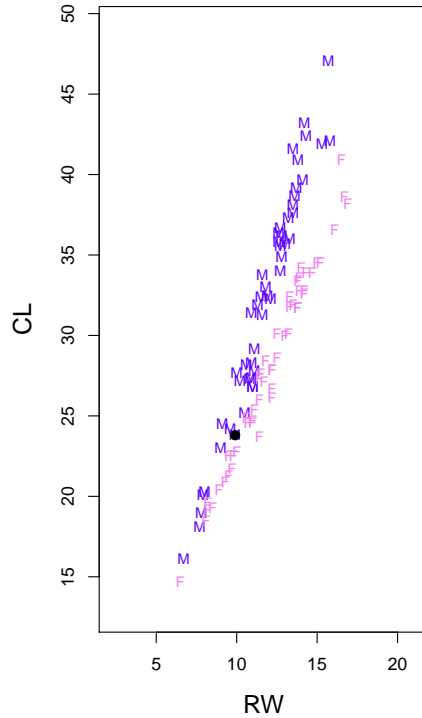


Figure 5: Blue crabs data: Scatterplot (F denotes female and M male; • denotes the observation perturbed for the analysis of Section 7.2).

Peel and McLachlan (2000), thirteen “perturbed” data sets are generated by substituting the original value of CL for the 7th point (highlighted by a bullet in Figure 5) with thirteen anomalous values shown in the first column of Table 10.

Ceteris paribus with Peel and McLachlan (2000), we directly fit the competing models with $G = 2$ clusters and in their VVV version only. Table 10 reports some of the obtained results. Note that the majority of the NCMs have not been fitted (refer to the missing values in Table 10) due to computational issues with the adopted R function `Mclust()`.

We firstly note that, for each approach, the BIC values deteriorate (increase) in line with the departure of the perturbed value from the bulk of the data; this is due to the log-likelihood part of the BIC. For the perturbed values of CL equal to -5, 0, 5, and 10, the lowest BIC values are obtained for NCMs; for the remaining perturbed values, the lowest BIC values are obtained for the tM . However, these are not the best approaches under other aspects. In particular, the CNM is systematically the most robust to the perturbations, with the number of misallocated observations remaining fixed at 12 regardless of the particular value perturbed (refer to the columns labeled as “#M”). This is especially in contrast to the NM, the NUM, and the NCM, where the number of misclassifications changes (and does not necessarily decrease) as the extent of the perturbation increases.

As concerns the fitted tMs and CNMs, the column labeled as “weight” denotes, in correspondence of the bad point and in its MAP cluster of membership, the weight assigned for parameter estimation; this weight is computed according to formula (19) for the CNM, and according to formula (7.22) in McLachlan and Peel (2000) for the tM . As expected, by recalling that the original value of CL for the 7th point was 23.8, these weights decrease as the CL value of the perturbed point further departs from its true value. A similar reasoning holds for the estimated degrees of freedom, in the cluster containing the bad point, for tMs (refer to the column labeled as “d.f.”) and for the estimated value of η_g , in the cluster containing the bad point, for CNMs (refer to the column labeled as “ $\hat{\eta}_g$ ”). In the former case,

CL	NM		tM					CNM					NUM				NCM								
	BIC	#M	BIC	#M	weight	d.f.	bad	#B	BIC	#M	\hat{v}_{τ_g}	weight	$\hat{\eta}_g$	bad	#B	BIC	#M	\hat{v}_{τ_g}	bad	#B	BIC	#M	\hat{v}_{τ_g}	bad	#B
-50	1071.19	20	968.53	13	0.0010	2.00	✓	9	969.41	12	0	0.0008	1284.41	✓	1	1005.22	14	0	✓	2					
-45	1066.56	20	967.99	13	0.0011	2.00	✓	9	969.14	12	0	0.0009	1119.84	✓	1	1005.05	13	0	✓	2					
-40	1061.47	21	967.41	13	0.0013	2.01	✓	9	968.84	12	0	0.0010	966.45	✓	1	1004.81	13	0	✓	2					
-35	1055.84	20	966.78	13	0.0016	2.04	✓	9	968.52	12	0	0.0012	824.20	✓	1	1004.40	13	0	✓	2					
-30	1049.54	18	966.09	13	0.0019	2.07	✓	9	968.18	12	0	0.0014	693.11	✓	1	1004.32	14	0	✓	2					
-25	1042.48	16	965.33	13	0.0023	2.10	✓	9	967.80	12	0	0.0017	573.17	✓	1	1003.38	34	0	✓	1					
-20	1034.56	16	964.49	13	0.0029	2.15	✓	9	967.38	12	0	0.0022	464.40	✓	1	1000.75	18	0	✓	1					
-15	1025.67	17	963.53	13	0.0037	2.20	✓	9	966.90	12	0	0.0027	366.78	✓	1	999.22	14	0	✓	1					
-10	1015.71	15	962.44	13	0.0049	2.26	✓	9	966.37	12	0	0.0036	280.31	✓	1	997.33	20	0	✓	1					
-5	1004.75	16	961.17	13	0.0068	2.34	✓	9	965.74	12	0	0.0049	204.99	✓	1	996.66	28	0	✓	1	948.96	13	0	✓	2
0	992.91	16	959.66	13	0.0100	2.45	✓	9	964.99	12	0	0.0071	140.83	✓	1	996.25	19	0	✓	1	947.63	13	0	✓	2
5	980.43	16	957.77	13	0.0161	2.60	✓	8	964.04	12	0	0.0114	87.77	✓	1	996.15	38	0	✓	1	945.77	13	0	✓	2
10	967.90	14	955.29	13	0.0297	2.85	✓	8	962.74	12	0	0.0219	45.59	✓	1	978.88	16	0	✓	1	942.44	14	0	✓	4

Table 10: Blue crabs data: Summary information about the fitted VVV models (“#M” = number of misallocations, without considering the true outlier; “weight” = weight given to the true outlier in the estimation of the parameters; “d.f” = estimated degrees of freedom, for the tM, in the cluster containing the true outlier; “#B” = number of detected outliers; “ \hat{v}_{τ_g} ” = probability for the true outlier to be a good point in the cluster g the outlier is assigned; “ $\hat{\eta}_g$ ” = estimated inflation parameter, for the CNM, in the cluster containing the true outlier). In the column labeled as “bad”, ✓ and ✗ indicate if the true outlier is detected or not, respectively, by the model.

this means that we need a t distribution with heavier tails as the bad point departs from the bulk of its cluster of membership; in the latter case, η_g can be also meant as a sort of “degree of badness”, i.e., as a measure of how different bad points are from the bulk of their cluster of membership.

In terms of outlier detection for the robust methods, we note that the probability to be a typical point for the bad point (refer to the columns labeled as “ \hat{v}_{τ_g} ”) is practically null for all of the approaches (such that this probability can be computed) regardless of the particular value perturbed. We can also note how all of the approaches are able to detect the bad point (refer to the columns labeled as “bad”); however, the CNM is the only model with a null FPR (refer to the columns labeled as “#B” reporting the number of detected outliers); this is especially in contrast to the the detection rule for tMs, based on the 95th percentile, which yields a number of detected bad points of either 8 or, in the majority of the cases, 9.

7.3. Wine data

The third analysis is based on the wine data set of Forina et al. (1998) available in the `gclus` package (Hurley, 2004) for R. These data comprise $p = 13$ physical and chemical properties of $n = 178$ wines grown in the same region in Italy but derived from three different cultivars (Barbera, Barolo, Grignolino). We treat this as a clustering analysis by ignoring the labels.

The competing families of parsimonious models are fitted for $G \in \{1, 2, 3, 4\}$. For each family, the best model, in terms of BIC, is reported in Table 11; the complete list of BIC values is given in Figure 6. Some of the BIC values are missing due to computational issues in estimating the corresponding model (see, in particular, Figure 6(d)).

Family of models	G	Parsimonious structure
NMs	3	VVE
tMs	4	VVI
CNMs	3	EEE
NUMs	4	VVI
NCMs	3	VVE

Table 11: Wine data: for each family of models, best number of clusters (G) and parsimonious covariance structure according to the BIC.

The clustering results (Table 12) show that the selected NM, CNM, and NCM recognize the presence of three clusters, while the remaining approaches find an additional (fourth) cluster. In terms of

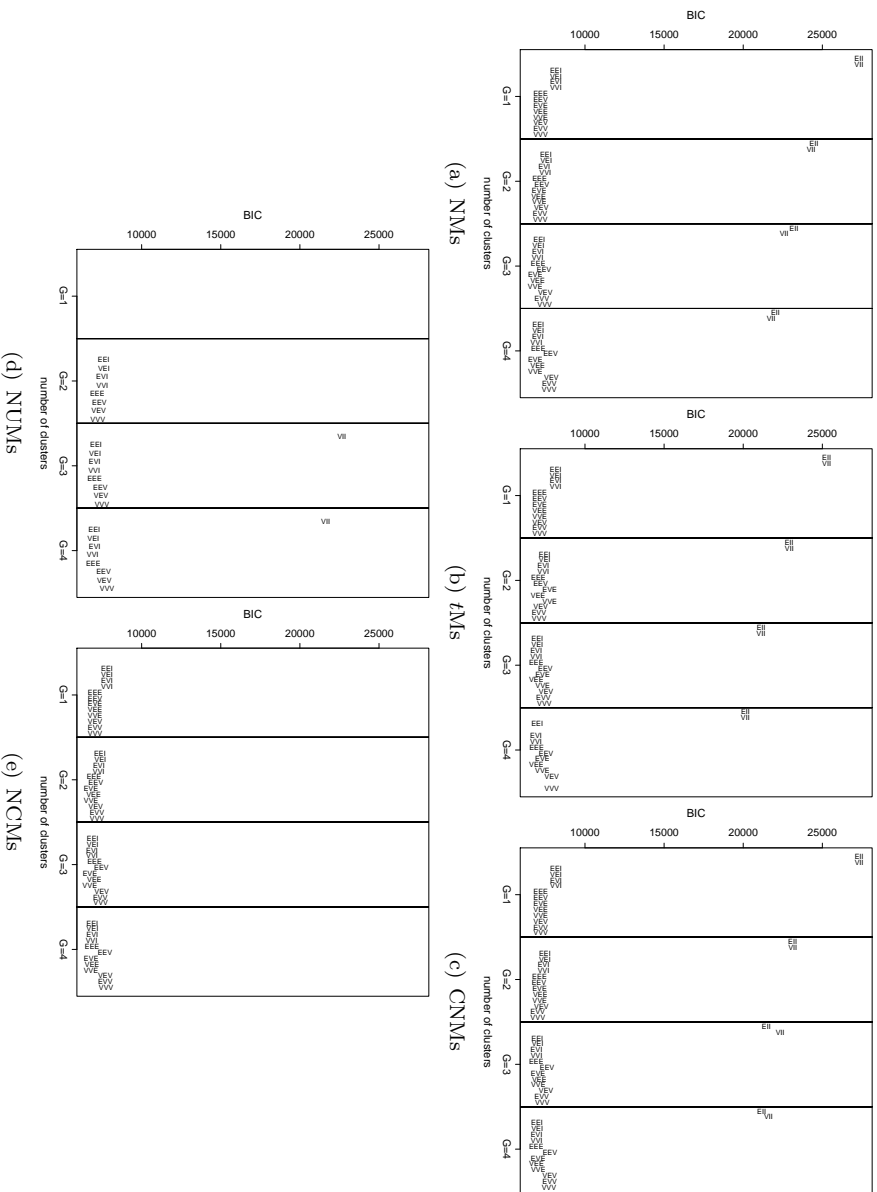


Figure 6: Wine data: BIC values for the fitted models.

	NM			tM			CNM			NUM			NCM		
	1	2	3	1	2	3	4	1	2	3	4	1	2	3	noise
Cultivar															
Barbera	48			48				48				48			
Barolo		59			34				25				58	1	58
Grignolino		2	4	65		5	55	11			2	48	21	1	60
															10

Table 12: Wine data: Clustering results for each of the competing methods, where good and bad samples are considered together for tMs, CNMs, and NUMs.

classification, the Barbera cultivar is classified correctly by all of the models. Instead, the Barolo and the Grignolino cultivars are classified correctly by the NCM only. Summarizing, only our approach leads to a perfect clustering when we consider the good points together with the bad points.

In terms of detection of bad points, the last part of Table 12 already reports the observations assigned to the noise component by the NCM. No bad points are detected by the NUM, while the observations declared as bad by the tM and the CNM are summarized in Table 13. We see that there are 35 bad points for the tM and 26 bad points for the CNM. Considering that Grignolino was the cultivar most difficult to be struggled by the competing methods (cf. Table 12), it is not surprising that the vast majority of bad points detected by the tM, the CNM, and the NCM, are in that cultivar. The graphical representation of the obtained classification for the CNM is shown in Figure 7.

Cultivar	tM					CNM			
	1	2	3	4	Bad	1	2	3	Bad
Barbera	42				6	44			4
Barolo		30		23	6		59		
Grignolino	1		45	2	23			49	22

Table 13: Clustering results for the PMCGD model on the wine data, where good and bad samples are considered separately.

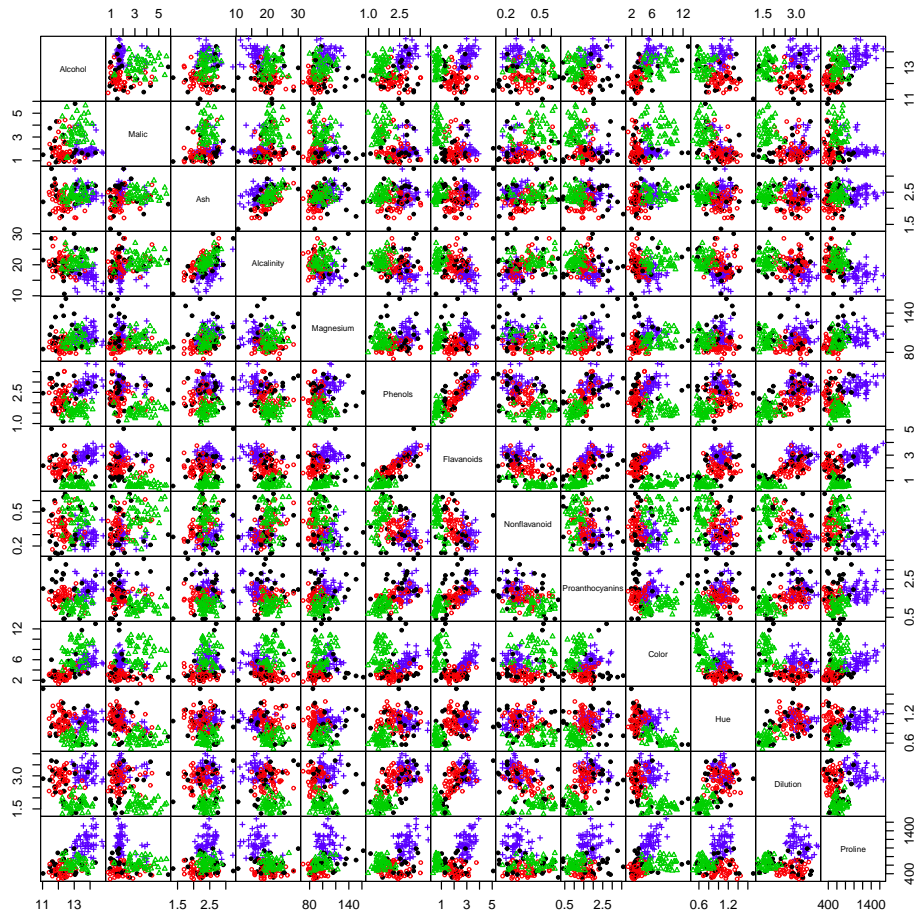


Figure 7: Wine data: Scatterplot matrix and clustering from the EEE-PMCGD model. Bad points are denoted by \bullet .

8. Discussion

A family of fourteen parsimonious mixtures of contaminated normal distributions has been introduced for clustering. These models can be viewed as an extension of the famous family of parsimonious mixtures of normal distributions introduced by Celeux and Govaert (1995). Firstly, as discussed in Section 5.5 and shown in the simulation study of Section 6, they facilitate robust estimation of model parameters in the presence of outliers, which we also refer to as bad points: as an example, the estimator of the cluster-specific mean vector in (16) is a weighted mean where the weights allow to reduce the impact of bad points in the estimation. Secondly, all of the members of our family of models allow for automatic detection

of bad points in the same natural way as observations are typically assigned to the groups in the finite mixture models context, i.e., based on the posterior probabilities of being good or bad points.

Another distinct advantage of our contaminated approach is that we can easily extend the approach to model-based classification (e.g., McNicholas, 2010) and model-based discriminant analysis (Hastie and Tibshirani, 1996). In fact, there are a number of options for the type of supervision that could be used in partial classification applications for our models, i.e., one could specify some of the $\{z_i\}_{i=1}^n$ and/or some of the $\{v_i\}_{i=1}^n$ *a priori*. This provides yet more flexibility than exhibited by any competing approach, as does the ability of our approach to work in higher dimensions where bad points cannot easily be visualized.

In all the considered data analyses of Section 7, and also in the simulations of Section 6, we demonstrated the good behaviour of our contaminated approach when compared to families of parsimonious: mixtures of normal distributions, mixtures of t distributions, mixtures of mixtures of a normal and a uniform distribution, and mixtures of normal distributions plus a uniform component.

As an open point for further research, it could be interesting to modify our approach with the aim of accommodating asymmetric contamination and/or “groups” of concentrated outliers. In such a case, contamination in the mean (and not in the covariance matrix, like we do) could be considered; see, e.g., the contaminated (location-shift) normal distribution considered by Verdinelli and Wasserman (1991).

Acknowledgments

A. Punzo acknowledges the financial support from the grant “Finite mixture and latent variable models for causal inference and analysis of socio-economic data” (FIRB 2012-Futuro in ricerca) funded by the Italian Government (RBFR12SHVV). P.D. McNicholas acknowledges the support of the Canada Research Chairs program. The authors finally declare the absence of any conflict of interest.

References

References

- Aggarwal, C. C., 2013. Outlier Analysis. Springer New York.
- Aitken, A., 1926. On Bernoulli’s numerical solution of algebraic equations. In: Proceedings of the Royal Society of Edinburgh. Vol. 46. pp. 289–305.
- Aitkin, M., Wilson, G. T., 1980. Mixture models, outliers, and the EM algorithm. *Technometrics* 22 (3), 325–331.
- Andrews, J. L., McNicholas, P. D., 2012. Model-based clustering, classification, and discriminant analysis with the multivariate t -distribution: The *tEIGEN* family. *Statistics and Computing* 22 (5), 1021–1029.
- Andrews, J. L., Wickins, J. R., Boers, N. M., McNicholas, P. D., 2015. *teigen*: Model-Based Clustering and Classification with the Multivariate t Distribution. Version 2.1.0 (2015-11-20).
URL <http://CRAN.R-project.org/package=teigen>
- Bagnato, L., Punzo, A., 2013. Finite mixtures of unimodal beta and gamma densities and the k -bumps algorithm. *Computational Statistics* 28 (4), 1571–1597.
- Bai, X., Yao, W., Boyer, J. E., 2012. Robust fitting of mixture regression models. *Computational Statistics & Data Analysis* 56 (7), 2347–2359.
- Banfield, J. D., Raftery, A. E., 1993. Model-based Gaussian and non-Gaussian clustering. *Biometrics* 49 (3), 803–821.
- Barnett, V., Lewis, T., 1994. Outliers in Statistical Data. Wiley Series in Probability & Statistics. Wiley.
- Becker, C., Gather, U., 1999. The masking breakdown point of multivariate outlier identification rules. *Journal of the American Statistical Association* 94 (447), 947–955.
- Berkane, M., Bentler, P. M., 1988. Estimation of contamination parameters and identification of outliers in multivariate data. *Sociological Methods & Research* 17 (1), 55–64.
- Biernacki, C., 2004. An asymptotic upper bound of the likelihood to prevent Gaussian mixtures from degenerating. Tech. rep., Université de Franche-Comté, Besançon.
- Biernacki, C., Celeux, G., Govaert, G., 2003. Choosing starting values for the EM algorithm for getting the highest likelihood in multivariate Gaussian mixture models. *Computational Statistics & Data Analysis* 41 (3-4), 561–575.
- Biernacki, C., Celeux, G., Govaert, G., Langrognet, F., Noulin, G., Vernaz, Y., 2008. MIXMOD - Statistical Documentation. Downloadable from http://www.mixmod.org/IMG/pdf/statdoc_2_1_1.pdf.
- Biernacki, C., Chrétien, S., 2003. Degeneracy in the maximum likelihood estimation of univariate Gaussian mixtures with EM. *Statistics & Probability Letters* 61 (4), 373–382.
- Bock, H. H., 2002. Clustering methods: From classical models to new approaches. *Statistics in Transition* 5 (5), 725–758.

- Böhning, D., 2000. Computer-assisted Analysis of Mixtures and Applications: Meta-analysis, Disease Mapping and Others. Vol. 81 of Monographs on Statistics and Applied Probability. Chapman & Hall/CRC, London.
- Böhning, D., Dietz, E., Schaub, R., Schlattmann, P., Lindsay, B., 1994. The distribution of the likelihood ratio for mixtures of densities from the one-parameter exponential family. *Annals of the Institute of Statistical Mathematics* 46 (2), 373–388.
- Böhning, D., Ruangroj, R., 2002. A note on the maximum deviation of the scale-contaminated normal to the best normal distribution. *Metrika* 55 (3), 177–182.
- Browne, R. P., McNicholas, P. D., 2014. Estimating common principal components in high dimensions. *Advances in Data Analysis and Classification* 8 (2), 217–226.
- Browne, R. P., McNicholas, P. D., 2015. *mixture: Mixture Models for Clustering and Classification*. Version 1.4 (2015-03-10). URL <http://CRAN.R-project.org/package=mixture>
- Browne, R. P., McNicholas, P. D., Sparling, M. D., 2012. Model-based learning using a mixture of mixtures of Gaussian and uniform distributions. *IEEE Transactions on Pattern Analysis and Machine Intelligence* 34 (4), 814–817.
- Browne, R. P., Subedi, S., McNicholas, P. D., 2013. Constrained optimization for a subset of the Gaussian parsimonious clustering models. arXiv.org e-print 1306.5824, available at: <http://arxiv.org/abs/1306.5824>.
- Byers, S., Raftery, A. E., 1998. Nearest-neighbor clutter removal for estimating features in spatial point processes. *Journal of the American Statistical Association* 93 (442), 577–584.
- Campbell, N. A., 1984. Mixture models and atypical values. *Mathematical Geology* 16 (5), 465–477.
- Campbell, N. A., Mahon, R. J., 1974. A multivariate study of variation in two species of rock crab of genus *Leptograpsus*. *Australian Journal of Zoology* 22 (3), 417–425.
- Celeux, G., Govaert, G., 1995. Gaussian parsimonious clustering models. *Pattern Recognition* 28 (5), 781–793.
- Celeux, G., Hurn, M., Robert, C. P., 2000. Computational and inferential difficulties with mixture posterior distributions. *Journal of the American Statistical Association* 95 (451), 957–970.
- Coretto, P., Hennig, C., 2011. Maximum likelihood estimation of heterogeneous mixtures of Gaussian and uniform distributions. *Journal of Statistical Planning and Inference* 141 (1), 462–473.
- Coretto, P., Hennig, C., 2015. Robust improper maximum likelihood: tuning, computation, and a comparison with other methods for robust Gaussian clustering. arXiv.org e-print 1406.0808, available at: <http://arxiv.org/abs/1406.0808>.
- Crawford, S. L., 1994. An application of the laplace method to finite mixture distributions. *Journal of the American Statistical Association* 89 (425), 259–267.
- Cuesta-Albertos, J. A., Gordaliza, A., Matrán, C., 1997. Trimmed k -means: An attempt to robustify quantizers. *The Annals of Statistics* 25 (2), 553–576.
- Davies, L., Gather, U., 1993. The identification of multiple outliers. *Journal of the American Statistical Association* 88 (423), 782–792.
- De Veaux, R. D., Krieger, A. M., 1990. Robust estimation of a normal mixture. *Statistics & Probability Letters* 10 (1), 1–7.
- Dempster, A. P., Laird, N. M., Rubin, D. B., 1977. Maximum likelihood from incomplete data via the EM algorithm. *Journal of the Royal Statistical Society: Series B (Statistical Methodology)* 39 (1), 1–38.
- Di Zio, M., Guarnera, U., Rocci, R., 2007. A mixture of mixture models for a classification problem: The unity measure error. *Computational Statistics & Data analysis* 51 (5), 2573–2585.
- Flury, B. N., Gautschi, W., 1986. An algorithm for simultaneous orthogonal transformation of several positive definite matrices to nearly diagonal form. *SIAM Journal on Scientific and Statistical Computing* 7 (1), 169–184.
- Forina, M., Leardi, R., Armanino, C., Lanteri, S., 1998. *PARVUS: An extendible package for data exploration, classification and correlation*. Tech. rep., Institute of Pharmaceutical and Food Analysis and Technologies, Genoa, Italy.
- Fraley, C., Raftery, A. E., 1998. How many clusters? Which clustering method? Answers via model-based cluster analysis. *Computer Journal* 41 (8), 578–588.
- Fraley, C., Raftery, A. E., Murphy, T. B., Scrucca, L., 2012. *mclust* version 4 for R: Normal mixture modeling for model-based clustering, classification, and density estimation. Technical report 597, Department of Statistics, University of Washington, Seattle, Washington, USA.
- Fraley, C., Raftery, A. E., Scrucca, L., Murphy, T. B., Fop, M., 2015. *mclust: Normal Mixture Modelling for Model-Based Clustering, Classification, and Density Estimation*. Version 5.1 (2015-10-27). URL <http://CRAN.R-project.org/package=mclust>
- Gallegos, M. T., Ritter, G., 2005. A robust method for cluster analysis. *The Annals of Statistics* 33 (1), 347–380.
- Gallegos, M. T., Ritter, G., 2009. Trimmed ML estimation of contaminated mixtures. *Sankhyā: The Indian Journal of Statistics, Series A* 71 (2), 164–220.
- García-Escudero, L. A., Gordaliza, A., 1999. Robustness properties of k means and trimmed k means. *Journal of the American Statistical Association* 94 (447), 956–969.
- García-Escudero, L. A., Gordaliza, A., Matrán, C., 2003. Trimming tools in exploratory data analysis. *Journal of Computational and Graphical Statistics* 12 (2), 434–449.
- García-Escudero, L. A., Gordaliza, A., Matrán, C., Mayo-Iscar, A., 2008. A general trimming approach to robust cluster analysis. *The Annals of Statistics* 36 (3), 1324–1345.
- García-Escudero, L. A., Gordaliza, A., Matrán, C., Mayo-Iscar, A., 2010. A review of robust clustering methods. *Advances in Data Analysis and Classification* 4 (2), 89–109.
- Gerogiannis, D., Nikou, C., Likas, A., 2009. The mixtures of Student’s t -distributions as a robust framework for rigid registration. *Image and Vision Computing* 27 (9), 1285–1294.
- Hartigan, J. A., 1985. Statistical theory in clustering. *Journal of classification* 2 (1), 63–76.
- Hastie, T., Tibshirani, R., 1996. Discriminant analysis by Gaussian mixtures. *Journal of the Royal Statistical Society: Series B* 58 (1), 155–176.

- Hathaway, R. J., 1986. A constrained EM algorithm for univariate normal mixtures. *Journal of Statistical Computation and Simulation* 23 (3), 211–230.
- Hawkins, D., 2013. *Identification of Outliers*. Monographs on Statistics and Applied Probability. Springer, The Netherlands.
- Hennig, C., 2002. Fixed point clusters for linear regression: computation and comparison. *Journal of Classification* 19 (2), 249–276.
- Hennig, C., 2004. Breakdown points for maximum likelihood estimators of location-scale mixtures. *The Annals of Statistics* 32 (4), 1313–1340.
- Hennig, C., Hausdorf, B., 2015. *prabclus: Functions for Clustering of Presence-Absence, Abundance and Multilocus Genetic Data*. Version 2.2-6 (2015-01-14).
URL <http://CRAN.R-project.org/package=prabclus>
- Holzmann, H., Munk, A., Gneiting, T., 2006. Identifiability of finite mixtures of elliptical distributions. *Scandinavian Journal of Statistics* 33 (4), 753–763.
- Hunter, D. R., Lange, K., 2000. Rejoinder to discussion of “optimization transfer using surrogate objective functions”. *Journal of Computational and Graphical Statistics* 9 (1), 52–59.
- Hurley, C., 2004. Clustering visualizations of multivariate data. *Journal of Computational and Graphical Statistics* 13 (4), 788–806.
- Ingrassia, S., 2004. A likelihood-based constrained algorithm for multivariate normal mixture models. *Statistical Methods and Applications* 13 (2), 151–166.
- Ingrassia, S., Rocci, R., 2007. Constrained monotone em algorithms for finite mixture of multivariate Gaussians. *Computational Statistics & Data Analysis* 51 (11), 5339–5351.
- Ingrassia, S., Rocci, R., 2011. Degeneracy of the EM algorithm for the mle of multivariate Gaussian mixtures and dynamic constraints. *Computational Statistics & Data Analysis* 55 (4), 1715–1725.
- Karlis, D., Xekalaki, E., 2003. Choosing initial values for the EM algorithm for finite mixtures. *Computational Statistics & Data Analysis* 41 (3–4), 577–590.
- Lebret, R., Iovleff, S., Langrognet, F., Biernacki, C., Celeux, G., Govaert, G., 2012. *Rmixmod: The R Package of the Model-Based Unsupervised, Supervised and Semi-Supervised Classification Mixmod Library*.
- Li, J., 2005. Clustering based on a multi-layer mixture model. *Journal of Computational and Graphical Statistics* 14 (3), 547–568.
- Little, R. J. A., 1988. Robust estimation of the mean and covariance matrix from data with missing values. *Applied Statistics* 37 (1), 23–38.
- Lo, Y., 2005. Likelihood ratio tests of the number of components in a normal mixture with unequal variances. *Statistics & Probability Letters* 71 (3), 225–235.
- Lo, Y., 2008. A likelihood ratio test of a homoscedastic normal mixture against a heteroscedastic normal mixture. *Statistics and Computing* 18 (3), 233–240.
- Lo, Y., Mendell, N. R., Rubin, D. B., 2001. Testing the number of components in a normal mixture. *Biometrika* 88 (3), 767–778.
- Markatou, M., 2000. Mixture models, robustness, and the weighted likelihood methodology. *Biometrics* 56 (2), 483–486.
- McLachlan, G., Krishnan, T., 2007. *The EM algorithm and extensions*, 2nd Edition. Vol. 382 of *Wiley Series in Probability and Statistics*. John Wiley & Sons, New York.
- McLachlan, G. J., Basford, K. E., 1988. *Mixture Models: Inference and Applications to Clustering*. Marcel Dekker, New York.
- McLachlan, G. J., Peel, D., 1998. Robust cluster analysis via mixtures of multivariate t -distributions. In: Amin, A., Dori, D., Pudil, P., Freeman, H. (Eds.), *Advances in Pattern Recognition*. Vol. 1451 of *Lecture Notes in Computer Science*. Springer, Berlin-Heidelberg, pp. 658–666.
- McLachlan, G. J., Peel, D., 2000. *Finite Mixture Models*. John Wiley & Sons, New York.
- McNicholas, P. D., 2010. Model-based classification using latent Gaussian mixture models. *Journal of Statistical Planning and Inference* 140 (5), 1175–1181.
- McNicholas, P. D., 2016. *Mixture Model-Based Classification*. Chapman & Hall/CRC Press, Boca Raton.
- McNicholas, P. D., Murphy, T. B., McDaid, A. F., Frost, D., 2010. Serial and parallel implementations of model-based clustering via parsimonious Gaussian mixture models. *Computational Statistics & Data Analysis* 54 (3), 711–723.
- Meng, X.-L., Rubin, D. B., 1993. Maximum likelihood estimation via the ECM algorithm: A general framework. *Biometrika* 80 (2), 267–278.
- Peel, D., McLachlan, G. J., 2000. Robust mixture modelling using the t distribution. *Statistics and Computing* 10 (4), 339–348.
- Punzo, A., Browne, R. P., McNicholas, P. D., 2016. Hypothesis testing for mixture model selection. *Journal of Statistical Computation and Simulation*. To appear, doi: 10.1080/00949655.2015.1131282.
- Punzo, A., Mazza, A., McNicholas, P. D., 2015. *ContaminatedMixt: Model-Based Clustering and Classification with the Multivariate Contaminated Normal Distribution*. Version 1.0 (2015-12-20).
URL <http://CRAN.R-project.org/package=ContaminatedMixt>
- R Core Team, 2015. *R: A Language and Environment for Statistical Computing*. R Foundation for Statistical Computing, Vienna, Austria.
URL <http://www.R-project.org/>
- Raftery, A. E., 1995. Bayesian model selection in social research. *Sociological Methodology* 25, 111–164.
- Ritter, G., 2015. *Robust Cluster Analysis and Variable Selection*. Vol. 137 of *Chapman & Hall/CRC Monographs on Statistics & Applied Probability*. CRC Press.

- Ruwet, C., García-Escudero, L. A., Gordaliza, A., Mayo-Iscar, A., 2012. The influence function of the tclust robust clustering procedure. *Advances in Data Analysis and Classification* 6 (2), 107–130.
- Ruwet, C., García-Escudero, L. A., Gordaliza, A., Mayo-Iscar, A., 2013. On the breakdown behavior of the tclust clustering procedure. *Test* 22 (3), 466–487.
- Schwarz, G., 1978. Estimating the dimension of a model. *The Annals of Statistics* 6 (2), 461–464.
- Stephens, M., 2000. Dealing with label switching in mixture models. *Journal of the Royal Statistical Society. Series B: Statistical Methodology* 62 (4), 795–809.
- Teicher, H., 1963. Identifiability of finite mixtures. *Annals of Mathematical Statistics* 34 (4), 1265–1269.
- Tukey, J. W., 1960. A survey of sampling from contaminated distributions. In: Olkin, I. (Ed.), *Contributions to Probability and Statistics: Essays in Honor of Harold Hotelling*. Stanford Studies in Mathematics and Statistics. Stanford University Press, California, Ch. 39, pp. 448–485.
- Verdinelli, I., Wasserman, L., 1991. Bayesian analysis of outlier problems using the Gibbs sampler. *Statistics and Computing* 1 (2), 105–117.
- Wolfe, J. H., 1965. A computer program for the maximum likelihood analysis of types. Technical Bulletin 65-15, U.S. Naval Personnel Research Activity.
- Yakowitz, S. J., Spragins, J. D., 1968. On the identifiability of finite mixtures. *The Annals of Mathematical Statistics* 39 (1), 209–214.
- Yao, W., 2012. Model based labeling for mixture models. *Statistics and Computing* 22 (2), 337–347.
- Yao, W., Wei, Y., Yu, C., 2014. Robust mixture regression using the t -distribution. *Computational Statistics & Data Analysis* 71, 116–127.